Aus dem Institut für Physiologie
der Medizinischen Fakultät Charité – Universitätsmedizin Berlin

DISSERTATION

Hyaluronan synthase 2 and hyaluronan in endothelial cells are increased by shear stress via the PI3-kinase-Akt-pathway with the most pronounced effect by an atheroprotective flow profile.

zur Erlangung des akademischen Grades
Doctor medicinae (Dr. med.)

vorgelegt der Medizinischen Fakultät
Charité – Universitätsmedizin Berlin

von

Julian Maroski

aus Berlin

Gutachter/in: 1. Prof. Dr. med. A. R. Pries

2. Prof. Dr. med. V. Djonov

3. Prof. Dr. G. W. Schmid-Schönbein

Datum der Promotion: 22.03.2013

1 Introduction 5

2 Material and Methods 9

2.1 Material 9

2.1.1 Chemicals and Buffers 9

2.1.2 Equipment 13

2.2 Methods 14

2.2.1 Cell culture 14

2.2.2 Shear stress 15

2.2.2.1 Application of constant shear stress 15

2.2.2.2 Application of pulsatile shear stress profiles 16

2.2.3 Cell treatment with inhibitors 19

2.2.4 RNA isolation and reverse transcription 20

2.2.5 Real-time quantitative PCR 20

2.2.6 Protein extraction and measurement 22

2.2.7 Antibodies 22

2.2.8 SDS PAGE and immunoblotting 22

2.2.9 Hyaluronan measurement 23

2.2.10 Immunofluorescence 23

2.2.11 Statistical analysis 24

3 Results 25

3.1 Endothelial hyaluronan synthase 2 expression 25

3.2 Modulation of hyaluronan synthase 2 expression by constant shear stress 27

3.3 Effect of pulsatile flow on endothelial hyaluronan synthase 2 30

3.4 Effects of PI3K- and Akt-inhibition on endothelial hyaluronan synthase 2 31

3.5 Effect of constant and atheroprotective shear stress on endothelial hyaluronan 34

3.6 Effects of PI3K-inhibition on hyaluronan in the ESL 35

4 Discussion 36

4.1 Main results and possible interpretations 36

4.2 Models for endothelial cells 36

4.3 Hyaluronan synthase 2 expression in unstimulated endothelial cells 37

4.4 Application of constant and pulsatile flow 38

4.5 Shear stress-dependent endothelial hyaluronan synthase 2 expression 39

4.5.1 Time-course 39

4.5.2 Force dependency 40

4.5.3 Pulsatile waveforms 41

4.5.4 Intracellular transduction pathways 41

4.6 Future prospects 42

4.7 Hyaluronan in the ESL: Regulation through shear stress 42

4.8 Expanding the picture of the endothelial surface layer 43

4.9 Summary and Conclusions 45

5 Abstract 46

6 Index of abbreviations 47

7 Index of figures and tables 49

8 References 50

List of publications 55

Erklärung 56

Lebenslauf 57

1 Introduction

Hyaluronan (HA), a highly negatively charged unsulfated glycosaminoglycan (GAG), consists of a linear chain of repeating disaccharides of N-acetylglucosamine (GlcNAc, figure 1) and glucuronic acid (GlcA, figure 1). Its molecular mass varies from 10^3 to 10^4 kDa, while the extended length ranges between two and 25 µm. Hyaluronan synthesis in mammals is catalysed in various cell types by one of three plasma membrane-bound hyaluronan synthases (HAS) at the inner face of the plasma membrane, each enzyme functioning independently as a synthase (1) (figure 1). Each single isoform of HAS protein is capable of hyaluronan biosynthesis. The three isoforms produce hyaluronan of different sizes: HAS1 and HAS2 synthesize large hyaluronan chains with higher molecular masses than those originating from HAS3 (figure 1, panel A) (1, 20). Especially HAS2 generates extremely long hyaluronan chains with an average molecular weight of even more than 2 x 10^3 kDa (20).

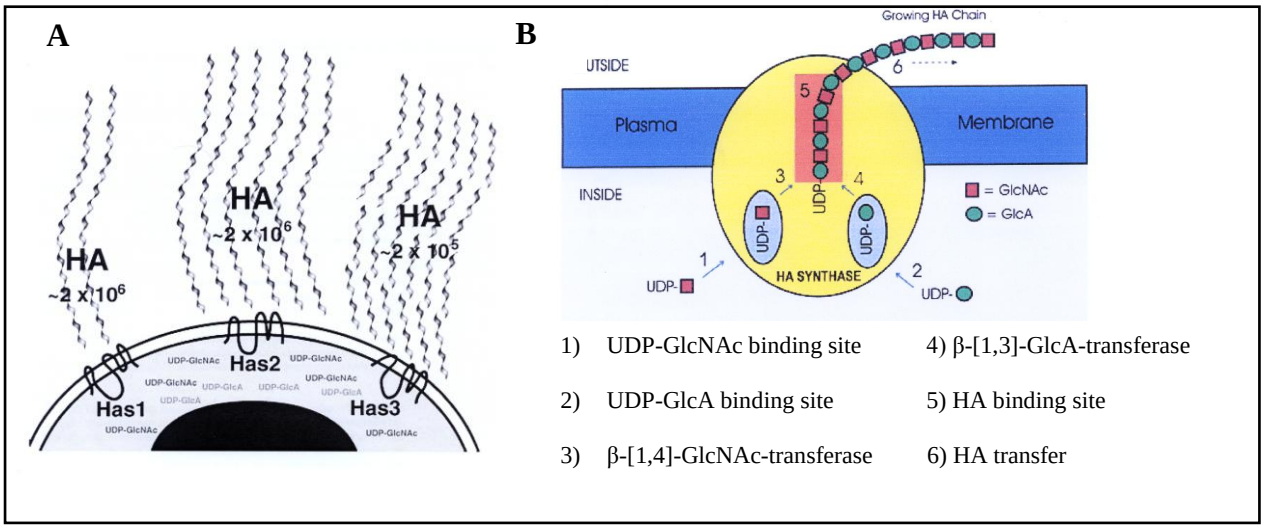

1) UDP-GlcNAc binding site
2) UDP-GlcA binding site
3) β-[1,4]-GlcNAc-transferase
4) β-[1,3]-GlcA-transferase
5) HA binding site
6) HA transfer

Figure 1) Scheme of distinct hyaluronan chain lengths and multiple functions of the three isoforms of hyaluronan synthases. *Panel A: production of hyaluronan (HA) with distinct chain lengths by the three isoenzymes of HA synthases (HAS) (1). Panel B: membrane bound streptococcal HAS with six enzyme functions needed to produce the disaccharide unit of HA and extend the growing chain. N-acetylglucosamine (GlcNAc), glucuronic acid (GlcA)* (51).

Unlike other GAG, extracellular HA is not attached to a core protein but remains attached to the enzyme (20) or binds to the hyaluronan binding protein CD44 or chondroitin sulphate,

respectively (45). For some decades hyaluronan has been regarded as a space filler in the extracellular matrix (25). Recently interest in hyaluronan has increased massively. It has been shown that hyaluronan is an essential molecule in various fields of biology, as in embryonic development, tissue organization in the intercellular matrix, wound healing, inflammatory processes, cancer biology and angiogenesis (1, 25). Hyaluronan associates with cell-surface receptors and can help to regulate cell motility and adhesion (1). Hyaluronan has been found to be present in the blood vessel wall, were it is produced by activated smooth muscle cells during arteriosclerosis in the neointima. There it accumulates during neointimal hyperplasia in association with smooth muscle cells (32) and may accelerate the development of arterisclerotic plaques (1). However, it has been assumed that hyaluronan has dual roles (32): it currently has been shown that hyaluronan is an important molecule to give structure to the endothelial surface layer (ESL) (42, 45, 50), and that hyaluronan in this surface structure is relevant for shear stress-induced endothelial NO-production (31, 35). Thus, hyaluronan in the ESL seems to be vasoprotective (33, 50) and important for vascular homeostasis (49).

Recent studies revealed that the inner blood vessel surface is lined with an endothelial surface structure, measuring at least 0.5 µm thick (15, 48, 49) and increasing with vascular diameter to more than 4.5 µm thick (38). Next to the glycocalyx, with some tens of nanometres (34, 37) various membranous glycoproteins, proteoglycans and glycosaminoglycans, like heparan sulfate (HS), chondroitin sulfate (CS) and hyaluronan, as well as associated macromolecules constitute the ESL (15, 45, 52). It is assumed that its physical properties, structure and thickness represent a steady state not only in terms of shedding into, and absorption from, the flowing blood but also of local synthesis of its components by endothelial cells (15, 38, 39, 52).

As the ESL constitutes the luminal aspect of the endothelium, it is important for the modulation of permeability in the transcapillary exchange of water as well as in controlling interactions of red and white blood cells with the endothelium (52). Due to its exposed position, the ESL provides an interface between the flowing blood and the vessel wall (35), which contributes to the transduction of shear stress into endothelial cells (35, 39, 40, 45). The ESL seems to be thicker at high shear stress regions with an undisturbed arterial flow profile, compared to vascular sites with lower shear stress (48, 54). The local thickness of the ESL and its structure are correlated with the laminar blood-flow generated shear stress acting on endothelial cells (50). The ESL in the carotid artery is reduced to less than 100 nm thick at regions with disturbed

blood flow. This reduction has also been found in an atheroprone mouse model with a high-fat, high-cholesterol diet (48). Both, disturbed blood flow and high-fat diet, result in higher levels of coagulation, inflammation and arteriosclerosis (45, 48). Degradation of the ESL allows platelet and leucocyte adhesion to the endothelial cells, which will set up an inflammatory reaction (34). Thus, it has been concluded that the ESL serves as an aegis, protecting blood vessels from coagulation and inflammation (45) and - especially at sites with undisturbed arterial blood flow - is one of the major factors defending the vessel wall against the development of arteriosclerotic plaques (16).

Although hyaluronan comprises only 5% to 25% of the GAG content in the ESL (45), it seems to have a significant structural role for the ESL. Treatment with hyaluronidase results in a reduction of the ESL in myocardial rat capillaries to less than 0.1 µm thick (50) and leaves a condensed stained layer resembling the glycocalyx, compared to a hairy structure of up to 0.5 µm thick in untreated vessels (figure 2). Furthermore, the endothelial nitric oxide (NO) release is reduced to about 20 % by this treatment, which results in impaired vessel dilatation properties (31). Consequently, removal of HA from the ESL is associated with reduced vascular dilatation properties, increased vascular vulnerability and endothelial dysfunction (33, 34).

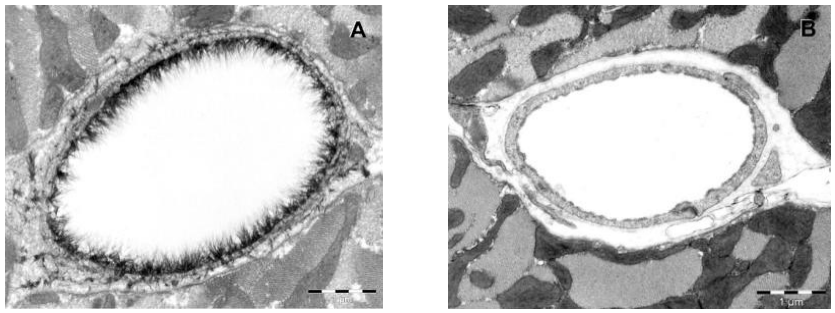

Figure 2) The ESL: Electron microscopy pictures of myocardial rat capillaries. *Both panels show electron microscopy pictures of an alcian blue 8GX stained rat myocardial capillary. Panel A: before treatment with hyaluronidase. Panel B: after hyaluronidase-treatment (50).*

In the last years, the role of the endothelium for the control and the regulation of vascular tone, coagulation and haemostasis, mainly effected through the active modulation of gene expression by shear stress, was investigated (2, 3, 8, 10). Recently, special interest has been aroused in different endothelial gene expression at vascular sites with high/low risk for arteriosclerosis, caused by different laminar/turbulent pulsatile shear stress waveforms (10). It has then been

shown that these different waveforms have indeed distinct effects on endothelial gene expression (10).

However, while all three hyaluronan synthase-isoforms are expressed in endothelial cells (44), and their expression has been found to be regulated by different growth factors and cytokines (1, 44), it is still not known whether these enzymes are influenced by shear stress. Based on its capacity to generate molecules with extremely large sizes (1, 20), the endothelial isoform 2 could be responsible for the observed incorporation of HA into the ESL under fluid shear stress conditions (15). This endothelial enzyme could help to explain the observed larger size of the surface layer at vascular sites that are exposed to undisturbed arterial blood flow, generating a pulsatile atheroprotective shear stress waveform.

To sum up, shear stress eminently modulates endothelial gene expression, endothelial cells actively regulate the GAG content on their surface (45, 52) and a major role of HA for the ESL serving as a shelter against arteriosclerosis has been shown. Therefore, the present study was designed to investigate the influence of shear stress on endothelial HAS2 expression in regard to cellular transduction pathways and with special interest in different shear stress waveforms. Particularly, a normal arterial flow profile was compared to a so called atheroprone pulsatile flow profile that continuously changed its direction, and the consequences of this on endothelial-generated HA were investigated.

2 Material and Methods

2.1 Material

2.1.1 Chemicals and Buffers

AGS GmbH, Heidelberg, Germany:

- Agarose

Amreso/Biometra GmbH, Göttingen, Germany:

- Acrylamid (38 %)

Appli Chem, Gatersleben, Germany:

- Marker II, prestained (6.5-200)

BD Biosciences, Heidelberg, Germany:

- anti-eNOS antibody (No. 610296)

Biochrom, Berlin, Germany:

- Collagenase type II from Clostridium histolyticum (0.2 %)
- Hank´s balanced salt solution (HBSS): 8 g NaCl, 0.4 g KCl, 0.14 g $CaCl_2$, 0.1 g $MgCl_2 \cdot 6\ H_2O$, 0.06 g KH_2PO_4, 1 g glucose, 0.02 g phenol red, 0.35 g $NaHCO_3$, 0.06 g $Na_2HPO_4 \cdot 2H_2O$ per 1 litre H_20.
- Phosphate buffered saline (PBS): 8 g NaCl, 0.2 g KCl, 0.1 g $CaCl_2$, 0.1 g $MgCl_2 \cdot 6\ H_2O$, 1.15 g $Na_2HPO_4 \cdot 2H_2O$, 0.2 g KH_2PO_4
- 0.05 % Trypsin/EDTA (500 U trypsin and 180 µg EDTA/ml in PBS)

Biorad, Munich, Germany:

- Bradford-Kit

Biozol, Eching, Germany:

- anti-ADAMTS-1 antibody (ab39194)

DAKO, Hamburg, Germany:

- Goat immunoglobulins (P0449)
- Mouse immunoglobulins (P0260)

Echelon Biosciences, Salt Lake City, USA:

- HA-ELISA-kit

Jackson Immunoresearch Laboratories, Suffolk, UK:

- Cy-3-conjugated goat-anti-rabbit and rabbit-anti-goat antibody

Kodak, Rochester, NY, USA:

- T-MAX developing kit and fixer

Merck Chemicals, Darmstadt, Germany:

- Akt-Inhibitor IV
- Bromophenol blue
- DTT
- Potassium chloride
- Potassium di hydrogen phosphate
- Sodium chloride
- Sodium di hydrogen phosphate
- Sodium phosphate

Perkin Elmer, Boston, MA, USA:

- Western lightning plus ECL detection kit

Promega, Madison, Wisconsin, USA:

- dNTP-Mix
- M-MLV Reverse Transcriptase
- oligo-dT-15-primer
- 5x RT buffer

PromoCell, Heidelberg, Germany:

- Cell-Growth-Supplement-Pack MV®
- Endothelial Cell Basal Medium MV®

Qiagen, Hilden, Germany:

- PCR Purification Kit
- QuantiTect SYBR Green PCR Kit
- Rneasy Mini Kit

Roth-Chemie GmbH&Co, Karlsruhe, Germany:

- Acetic acid
- Ammoniumperoxydisulfate (APS)
- Ethanol (70 % and 95 %)
- Glycine
- Methanol
- Tricine
- Tris

Santa Cruz Biotechnologies, Heidelberg, Germany:

- anti-HAS2 antibody (Sc-34067)
- anti-HAS2 antibody (Sc-66916)
- anti-PECAM-1 antibody (Sc-1506)
- Blocking peptide (Sc-34067P)

Sigma-Aldrich, Taufkirchen, Germany:

- BSA
- SDS
- Dextrane

- LY294,002
- Monoclonal β-actin antibody (AC 15, A 5441)

Sucofin, Zeven, Germany:

- Milk powder, 0.9 % fat

Anode buffer:

- 0.2 M tris-HCL pH 8.9

Extraction buffer:

- 1% (w/v) triton x-100, 20 mmol/L sodium-phosphate-buffer (pH 7.8), 150 mmol/L sodium chloride, 2.5 mmol/L EDTA, 1 mmol/L sodium vanadate, 50 mmol/L sodium fluoride, 1 mmol/L phenylmethylsulfonyl fluoride, 0.02 µg/µL aprotinin, 0.02 µg/µL leupeptin and 0.02 µg/µL pepstatin A

Cathode buffer:

- 35.84 g tricine, 24.22 g tris, 20 mL 10% SDS per 2 L H_2O

Gel preparation:

- stock solutions: A) 121.9 g acrylamide, 3.13 g DAP per 250 ml H_2O; B) 18.15 g tris per 100 mL H_2O (pH 8.8); C) 12.1 g tris per 100 mL H_2O (pH 6.8)
- 10% APS, TEMED, 10% SDS

Laemmli sample buffer:

- 50 mmol/L sodium-phosphate, 100 mmol/L DTT, 2 % SDS, 10 % glycerol and 0,1 % bromophenol blue

Transfer buffer:

- 3 g tris, 11.2 g glycin, 100 mL methanol per 1 L H_2O

Washing buffer:

- 0.1 % v/v Tween 20 in PBS, pH 7.2

2.1.2 Equipment

Amersham, Buckinghamshire, United Kingdom:

- GeneQuant photometer
- Hyperfilm ECL

Becton Dickinson, Franklin Lakes, New Jersey, USA:

- Primaria® culture dishes (100 x 20 mm)

Biometra, Göttingen, Germany:

- Standard Power Pack P25
- UNO-Thermoblock

Biorad, Munich, Germany:

- Mini Protean 3 System: glass plates, spacer plates
- Tank blot chamber-system

Branson Sonic Power Company, Danbury, Connecticut, USA:

- Sonifier B-12 Cell Disruptor

Canon, Tokyo, Japan:

- Canon EOS 10D

Eppendorf, Hamburg, Germany:

- Centrifuge 5417R
- Photometer 1101M
- Safe Seal Micro Tubes

Faulhaber, Stuttgart, Germany:

- DC motor 1624 E, 1,84W and 3863024C, 197 W
- Reduction gear 1/12 and 41/1

Heraeus, Hanau, Germany:

- Biofuge stratos centrifuge

- Incubator B 5060 EK/CO_2
- Workbench HS 12

Heidolph, Schwabach, Germany:

- Titramax 1000, rocking platform

Leitz, Wetzlar, Germany:

- Ortholux microscope
- Objective (25/0.60 W FLUORESZENZ)
- Filter set N2.1

LTF, Wasserburg, Germany:

- Rotor Gene 2000 cycler

Sarstedt, Nürnbrecht, Germany:

- Tissue culture flasks

Scanalytics, Rockville, USA:

- One dscan

Techne, Wertheim, Germany:

- Dri-Block DB2A

Whatman, Dassel, Germany:

- Protran BA 83 nitrocellulose membranes, 0.2µm, 200 mm x 3 m

2.2 Methods

2.2.1 Cell culture

Human umbilical vein endothelial cells (HUVEC) were isolated as previously described (2, 21). After separation from the placenta, human umbilical cords were kept at 4°C for at most 24 hours. HUVEC were removed from umbilical veins of umbilical cords, after rinsing with 20 mL of PBS, with 8 mL 0.2 % collagenase type II from Clostridium histolyticum by incubating them for

15 minutes at 37°C. After the incubation the respective veins were rinsed with 20 mL phosphate buffered saline (PBS). HUVEC were washed out, the suspension was collected and centrifuged for 5 minutes at room temperature with 1,500 × *g* to pelletise the cells. Next, HUVEC were re-suspended in 10 mL culture medium and seeded into tissue culture flasks. Cells were cultivated to confluence at 37°C in a humidified atmosphere with 5% CO_2. Then during their first-passage, HUVEC were seeded on two to four Primaria® culture dishes. These first passage cells were used for shear stress experiments one day after confluence.

2.2.2 Shear stress

2.2.2.1 Application of constant shear stress

HUVEC were exposed to constant shear stress using a cone-and-plate system as previously described (2, 3). This apparatus was build with a lower platform, supporting the shear cone arrangement, including a sliding table to position the culture dish with the HUVEC. An upper platform supported a DC motor (1624 E, 1,84W) with a 41/1 reduction gear, that transmitted the rotation via a driving belt and a shaft to a constantly rotating replaceable, stainless cone. The cone fits standard petri dishes with a diameter of 100 mm. The apparatus was placed in an incubator that provided the cells with the humidified atmosphere with 5 % CO_2 at 37°C. For experiments, the sliding table with the petri dish was moved up to the working position, so that the cone tip was just touching the center of the culture dish. To control its position, three stop screws were adjusted to guarantee the adjustment of the dish. The cone was inserted into the 100-mm culture dish providing uniform shear stress (τ) over the entire cross-sectional area, according to:

$$\tau = (\omega/\alpha) \times \eta,$$

with τ (dyn·cm^{-2}) being the shear stress, ω (rad·s^{-1}) the angular velocity, α (rad) the cone angle (1°) and η (dyn·s·cm^{-2}) the fluid viscosity. The angular velocity and the medium viscosity were altered in order to achieve the appropriate shear stress with constant laminar flow. The characteristics of the flow could be defined in analogy to Reynolds (6), according to:

$$R = r^2\omega\alpha^2 / 12\upsilon,$$

with υ being the kinematic viscosity calculated through η/ρ. For $R < 1$ shear stress was assumed to be laminar, for $R \geq 1$, flow was assumed to be turbulent (see 2.2.2.2). In the described system

r was 0.05 m, η was 0.75 cPoise, ρ was 1000 kg/m^3 and ω was 14.03 s^{-1}. So that R was calculated 0.84, which meant flow was not turbulent. In this study HUVEC were exposed to constant laminar flow generating shear stress of 2 dyn/cm², 6 dyn/cm², 10 dyn/cm² and finally of 20 dyn/cm² (figure 3). These shear stress values were regarded as "applied shear stress" on the endothelial surface layer, acting on the rotating cone. In order to keep flow conditions laminar in samples being exposed to higher shear stress than 6 dyn/cm², medium viscosity was increased to 5 cPoise by adding 83 mg dextrane per mL medium (personal communication R. Knudsen). Control samples from the same isolation were kept simultaneously under same conditions without flow.

2.2.2.2 Application of pulsatile shear stress profiles

Next to constant flow, two large arterial flow profiles, measured in human carotids, as recently described by Dai et al. (10), were applied to HUVEC in this study. Briefly, Dai transferred hemodynamic conditions measured non-invasively via MRI in normal human carotids to an *in vitro* model. Two prototypical shear stress waveforms from two anatomical locations were selected: Firstly from the internal distal carotid, secondly from the carotid sinus. Even though these two sites are located close to each other, they were found to have distinct hemodynamics and different addictions to develop atherosclerotic lesions. The shear stress waveforms of these two locations were analysed and transferred to an *in vitro* model using a special cone-and-plate system. According to their characteristics, to protect the vessel wall from arteriosclerosis, or to forward arteriosclerosis, they were called "atheroprotective" and "atheroprone", respectively. The atheroprotective shear stress waveform was preferentially found at the distal inner carotid and was seen as a prototype for normal arterial flow. Shear stress at these sites averages values between 4 and 16 dyn/cm². Accordingly, shear stress waveforms from this site only vary in respect to the mean value, while they are rather similar to each other in respect to their hemodynamics. Thus, Dai selected a midranged shear stress waveform. In contrast, atheroprone shear stress waveforms are seen at sites with a high probability of arteriosclerosis plaque development with a larger heterogeneity.

In the present study, the atheroprone flow profile was characterised by shear stress ranging from -8.9 to 3.7 dyn/cm^2 and the atheroprotective profile by shear stress ranging from 13.3 to 43.7 dyn/cm^2 (figure 3). These profiles vary with respect to different parameters, as the mean

shear stress (τ_{mean}), shear stress amplitude (τ_{ampl}), maximal rate of change in shear stress ($d\tau/dt_{max}$, $d\tau/dt_{min}$) and the direction of shear stress.

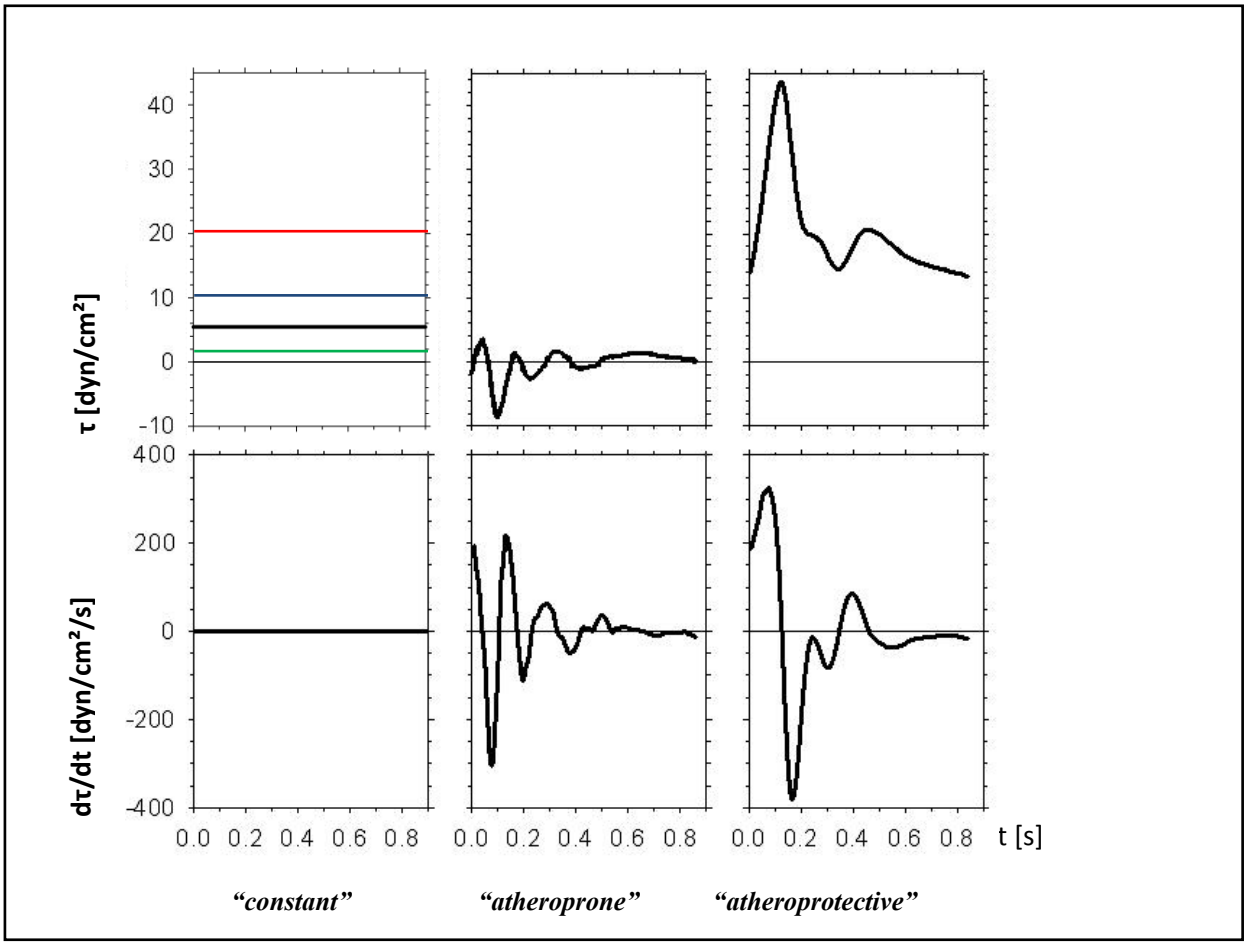

Figure 3) Shear stress patterns of constant and pulsatile laminar shear stress waveforms. *For the vascular shear stress patterns used in this study, shear stress (τ, upper panels) and the rate of change in shear stress (dτ/dt, lower panels) are shown over one heart cycle. In this study constant shear stress of 2 dyn/cm² (green line), of 6 dyn/cm² (black line), of 10 dyn/cm² (blue line) and of 20 dyn/cm² (red line) was applied to the HUVEC. The major characteristics of the atheroprotective profile is high pulsatile shear stress with fast acceleration and deceleration. The characteristic of the atheroprone profile is low mean shear stress, but marked oscillations between antegrade and retrograde flow with fast acceleration and deceleration.*

HUVEC were exposed to these flow profiles using a cone-and-plate-system with a microprocessor, which controlled the rotational speed of the cone, and a stronger motor (3863024C, 197 W), which made it possible to achieve acceleration speeds of real blood flow profiles (figure 4). This combination allowed a maximal rotational speed of 430 rpm. The rotation was transmitted directly by a shaft to the cone in order to reduce the inertia of the

system. The power supply and motor control was realized by a control box which was loaded with the desired velocity profile via a serial link from a personal computer.

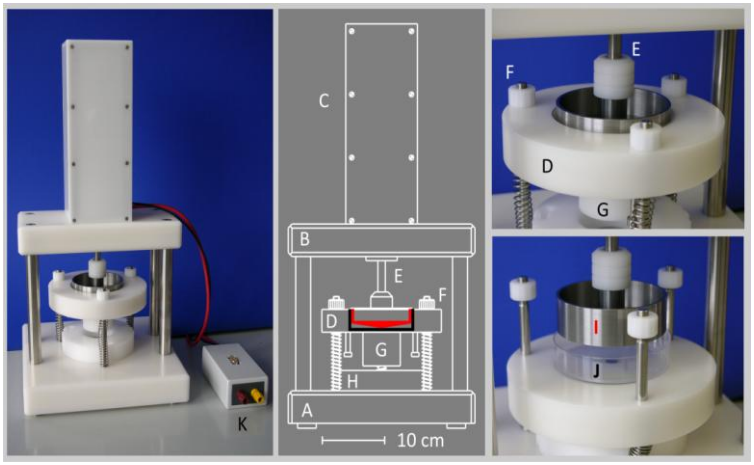

Figure 4) General outline of the cone-and-plate-system to simulate pulsatile flow. *The lower platform (A) carries the shear cone arrangement (E-J), while the upper platform (B) supports a strong DC motor in a shielded housing (C). The motor rotates the interchangeable cone (I, red in middle panel) via transmission of a shaft (E). The cone is inserted into the petri dish (J, black in middle panel) by lifting the sliding table (D), fixed with a rotating disc (H), to its upper working position (left panels). To control this position, three stop screws (F) are adjusted, and the final position is defined by establishing electrical contact between the cone and a metal plate in the center of the culture dish support (G). The pulsatile flow profiles are loaded by a computer into the motor control box (K).*

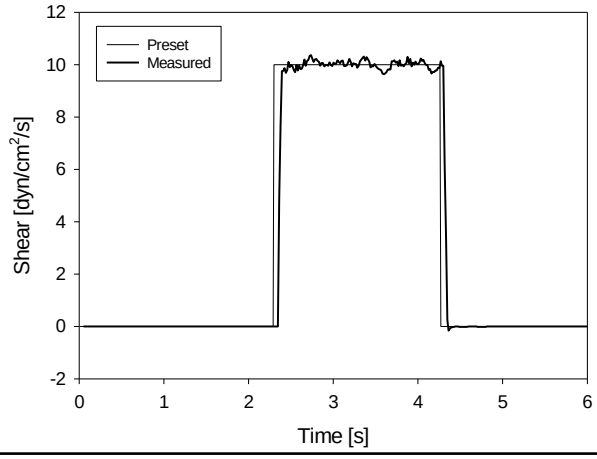

Figure 5) Reproduction of flow patterns with the second cone-and-plate device. *Performance characteristics of the pulsatile cone-and-plate system. The figure shows desired (thin line) and actual (fat line, shifted by 50 ms to the right) patterns of rotational velocity (or shear). The actual data were measured outside the shear cone.*

To avoid a cell damage after an abrupt switch from static to shear conditions, the motor control software provided conditioning sequences during which the rotational speed was continuously increased from zero to the average speed of the shear pattern to be used. This cone-and-plate-system allowed a close reproduction of the flow patterns, even with high acceleration rates (figure 5). Dextrane was added to the medium in order to increase the viscosity of the flowing medium to guarantee laminar flow conditions at higher shear stress conditions. Again, the control samples from the same isolation were kept simultaneously under the same culture conditions but without flow. Different morphological effects of atheroprotective and atheroprone shear stress waveforms could be observed through the microscopy, thus validating the concept of application of flow profiles (figure 6).

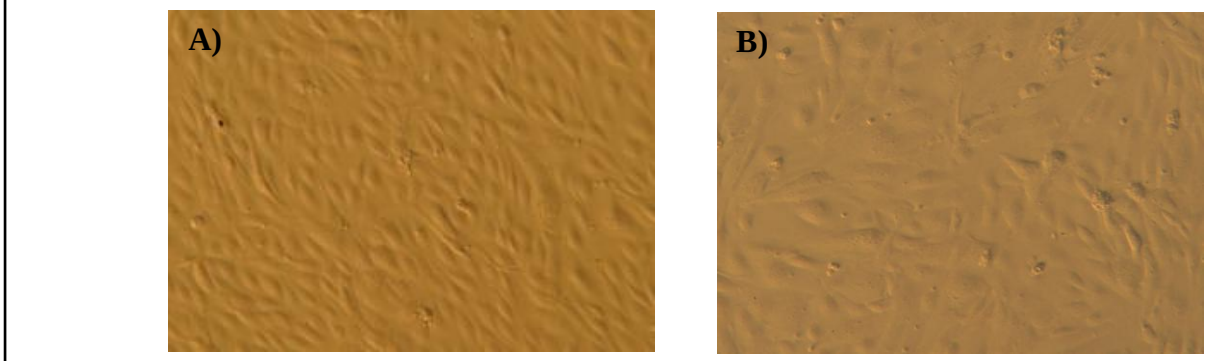

Figure 6) Cell shape and alignment after exposure to pulsatile shear stress profiles. *HUVEC were either exposed to atheroprotective pulsatile flow (shear stress between 13.3 and 43.7 dyn/cm^2) (panel A) or to atheroprone pulsatile flow (shear stress between -8.9 and 3.7 dyn/cm^2) (panel B) for 24 hours. Pictures were taken with a Canon EOS 10D.*

2.2.3 Cell treatment with inhibitors

Phosphatidylinositol 3-kinase (PI3K) was inhibited using LY294,002. A stock solution (10 mmol/L) was prepared in dimethylsulfoxide (DMSO) and used at a final concentration of 10 µmol/L, hence the respective final dilution of DMSO was 1:1000. RAC-alpha serine/threonine-protein kinase (Akt) was inhibited using Akt-Inhibitor IV in a final concentration of 5 µmol/L, thus the final dilution of DMSO was 1:2000. Cells were pre-incubated with the respective inhibitors for 30 minutes and then exposed to shear stress as described above.

2.2.4 RNA isolation and reverse transcription

HUVEC were harvested with 0.05% trypsin / EDTA pelletised and frozen in liquid nitrogen at -196 °C. RNA was isolated with the Rneasy Mini Kit according to the manufacturer's protocol. Briefly: cells were homogenised, lysed, pipetted onto a column and centrifuged, so that the RNA was bound to a silica-gel membrane. After washing, the RNA was eluted with 40 µL of RNase-free water. The amount of resulting RNA was estimated with a GeneQuant photometer at 260 nm. 2 µg of total RNA and 1 µg of oligo-dT-15-primer in a total volume of 15 µL were heated (70 °C, 8 min) in an UNO-Thermoblock to denaturate the RNA and afterwards cooled on ice. 200 U M-MLV Reverse Transcriptase, 1.25 µL dNTP-Mix 10 mM and 5 µl 5x RT buffer were added to a total volume of 25 µL, then incubated at 42 °C (1 h) and finally the enzyme was inactivated (70 °C, 10 min). 18 µL DEPC-treated water (H_2O_{DEPC}) was added and aliquots of 1 µL were used as template in the Polymerase Chain Reaction (PCR).

2.2.5 Real-time quantitative PCR

All nucleotide sequences used refer to the "Entrez Nucleotides" - database of the National Center for Biotechnology Information (NCBI; Bethesda, USA, http://www.ncbi.nlm.nih.gov/). For producing cDNA consisting of 250 to 800 base pairs (bp), usable as a template for external standards, primer pairs were searched with "Primer3" at Whitehead Institute for Biomedical Research (Massachusetts, USA, http://www.wi.mit.edu/) and their selectivity was tested with the BLAST programme of the NCBI. The following primer pairs were used (Table 1):

Table 1) Primers taken to produce template-cDNA.

Gene	Primer pairs	Annealing temperature	Product size
HAS2, accession NM_005328	gatggctaaaccagcagacc ggttttccttcctgatgtgc	56 °C	374 bp
GAPDH, accession NM_002046	cctgacctgccgtctagaaa tactccttggaggccatgtg	56°C	276 bp

Primers in a final concentration of 0.3 µmol/L were added to 1 µL cDNA template, 10 µL master mix and nuclease-free water to a total volume of 20 µL. The PCR, performed in a Rotor Gene 2000 cycler, was started at 94 °C for 900 s. 40 cycles followed, each consisting of a sequence of denaturation (94 °C for 15 s), annealing (56 °C, 30 s) and elongation (72 °C, 75 s). The purity of the amplification products was ensured by melting curve analysis. Non-RT- and non-template controls were run for all reactions. The amplification products were separated in agarose/ethidium bromide-gels (2% agarose and 1‰ ethidium bromide in 1x Tris/Borate/EDTA-Buffer (TBE)) and visualised at 254 nm to ensure their purity and correct length. The products were purified using the QiaQuick PCR Purification Kit according to manufacturer's protocol. Briefly: the samples were diluted and applied onto a spin column, washed, and the cDNA was eluted. Its concentration was measured at 260 nm. The quantity of copies was calculated according to:

$$\text{concentration [molecules/µL]} = (\text{concentration [µg/mL]}) / (\text{product length [bp]} \times 660) \times 6{,}022 \cdot 10^{14}$$

In dilutions from 10^8copies/µL to 10^2copies/µL, the 250 – 800 bp long products were used as a template to generate standard curves for real-time quantitative (rtq) PCR. In this rtq-PCR, product sequences with a length of 100 – 200 bp were generated which represent a part of the respective 250 – 800 bp product. The following primer pairs were used (Table 2):

Table 2) Primers taken for real-time quantitative PCR.

Gene	Primer pairs	Annealing temperature	Product size
HAS2	accggggtaaaatttggaac	58 °C	162 bp
	acatcttggcgggaagtaaa		
	gtggctccagttggaattgt		
GAPDH	tcaagaaggtggtgaagcag	56°C	198 bp
	ccctgttgctgtagccaaat		

40 cycles were run in the real-time cycler as described above. Non-template controls were run for all reactions as a negative control.

2.2.6 Protein extraction and measurement

HUVEC were cooled on ice, suspended with a cell scraper in 250 µL extraction buffer (see 2.1.1) and than homogenized on ice, using a syringe with a needle (0.4 mm x 19 mm), followed by sonification. Homogenates were centrifuged (20 000 × *g* for 10 minutes, 4 °C), supernatants transferred into a fresh tube, and protein concentrations were determined with Bradford-Kit. Briefly, this kit is based on the principle, established by Bradford (5): Coomassie brilliant blue G-250 is bound to proteins, which leads to a shift in the maximum absorption of protein-bound coomassie brilliant blue to 595 nm. The amount of protein in the samples can be determined with the help of the increased absorption at 595 nm measured in a photometer using a standard curve produced with known amounts of protein. This method was chosen because of its rapidity, high sensitivity (1 µg protein) and its slight chemical interference, which allowed using it in the presence of the extraction buffer described above.

2.2.7 Antibodies

Antibodies were used for immunoblotting, detecting HAS2 in a dilution of 1:700, PECAM-1 (platelet endothelial cell adhesion molecule) in a dilution of 1:15,000, ADAMTS-1 in a dilution of 1:2,000, eNOS in a dilution of 1:4,000 and β-actin in a dilution of 1:12,000. As a negative control blocking peptide was combined in a five-fold excess with the respective antibody and incubated over night at 4 °C. Next day this solution was used for immunoblotting under the same conditions as the investigated HUVEC-samples.

2.2.8 SDS PAGE and immunoblotting

Forty micrograms of cell extracts were mixed with Laemmli sample buffer, heated at 95 °C for 3 minutes and then loaded on a gel (stacking gel 5% acrylamide, resolving gel 7-10% acrylamide). Proteins were separated using the sodium-dodecyl-sulfate polyacrylamide gel-electrophoresis (SDS-PAGE) described by Laemmli (23). After separation of proteins by SDS–PAGE, proteins were transferred to nitrocellulose membranes in tank blot chambers. These membranes were then blocked with 5% (w/v) low-fat, dry milk powder in washing buffer at 4 °C over night. Next day blot membranes were incubated with primary antibodies for 2 hours at

room temperature and subsequently, after 30 minutes of washing, for 60 minutes with a peroxidase-conjugated secondary antibody, in a dilution of 1:5,000. Unbound secondary antibodies were removed by five incubations (6 minutes each) in washing buffer. Equal protein loading was confirmed by Ponceau staining and PECAM-1 expression. For ADAMTS1 blots protein loading was confirmed by β-actin expression, due to the molecular weight of ADAMTS1. Immunoblots were developed by chemiluminescence using an ECL detection kit visualised by exposing blots to Hyperfilm ECL for varying times, and scanned for densitometric and molecular weight quantification with ONE-Dscan.

2.2.9 Hyaluronan measurement

Hyaluronan content was determined by using an enzyme-linked immuosorbent assay (ELISA) kit which was designed for *in vitro* measurement of HA levels in diverse biological fluids. The principle is based on a competitive ELISA in which the colorimetric signal is inversely proportional to the amount of hyaluronan in the sample. The concentration of HA in the samples is determined by using a standard curve of known amounts of hyaluronan. For hyaluronan measurement, cells were exposed to pulsatile laminar atheroprotective flow, as described above, as well as to constant laminar flow for 24 h or were kept under non-flow control conditions. HUVEC were harvested with 2 ml 0.05% trypsin / EDTA for 30 minutes at room temperature and subsequently for another 10 minutes at 37 °C. Cells, which were not detached after 40 minutes of incubation in trypsin / EDTA, were suspended with a cell scraper. Afterwards this suspension was centrifuged for 5 minutes at room temperature at 1,500 × *g* to separate the cells from the trypsinated fraction (ESL) (15). Next, cells were re-suspended in 2 mL PBS and counted in a Neubauer chamber (0.1 mm depth). Next, the two fractions were analysed with the ELISA kit. The calculated amount of hyaluronan in supernatant and trypsinated glycocalyx-fraction was then related to the cell number per petri dish.

2.2.10 Immunofluorescence

Confluent cells were fixed with methanol at –20 °C for 10 minutes. Afterwards they were washed in PBS with 1 % BSA and incubated with two different anti-HAS2 antibodies (Sc-34067 and Sc-66916) each in a 1:150 dilution in PBS/BSA for 30 minutes at room temperature to detect

HAS2 protein. They were then washed twice in PBS with 1 % BSA and incubated with Cy-3-conjugated goat-anti-rabbit and rabbit-anti-goat antibody respectively each in a 1:1,000 dilution in PBS with 1 % BSA for another 30 minutes. Again they were washed two times with PBS/BSA and directly analysed using an Ortholux microscope equipped with a water immersion objective (25/0.60 W FLUORESZENZ), and filter set N2.1 for epi-fluorescence. Photos were taken with constant time exposure using a Canon EOS 10D. Negative control was done by using the respective secondary antibody only for analysis.

2.2.11 Statistical analysis

"*n*" refers to the number of umbilical cords from which HUVEC had been isolated. Cells from the same umbilical cord were distributed to two to four petri dishes and either exposed to enzyme inhibitors or cultured without and subsequently placed in the cone-and-plate system or kept as static control. Data are given as means ± standard error mean (SEM), from (n) independent experiments, as indicated. Statistical analysis was done using Student's two-tailed *t*-test for paired samples if cells came from the same umbilical cord or for unpaired samples when they came from different cords. The statistical significance was set at a value of $p \leqslant 0.05$ (*), high significance was set as a value of $p \leqslant 0.01$ (**).

3 Results

3.1 Endothelial hyaluronan synthase 2 expression

Initially, HUVEC were cultured for 24 h in control conditions without shear stress and were analysed for HAS2 protein expression by immunoblotting (figure 7) and by immunofluorescence (figure 8). In order to analyse the expression of HAS2 protein, two different methods of protein extraction for immunoblotting were performed. Either HUVEC were directly extracted into Laemmli sample buffer at 96 °C, or cells were extracted into the extraction buffer (see 2.1.1 and 2.2.6). Afterwards the cell lysates were loaded on a gel as described. While cell lysates of HUVEC, extracted into the extraction buffer, showed two different bands (at a molecular weight of about 43 kDa and 65 kDa), cell lysates of HUVEC directly extracted into Laemmli sample buffer contained the upper band only (figure 7). Figure 7 shows the immunoblotting of HAS2 including the upper part of the membrane with the 116 kDa range, which is used for PECAM-1 as loading control in other experiments.

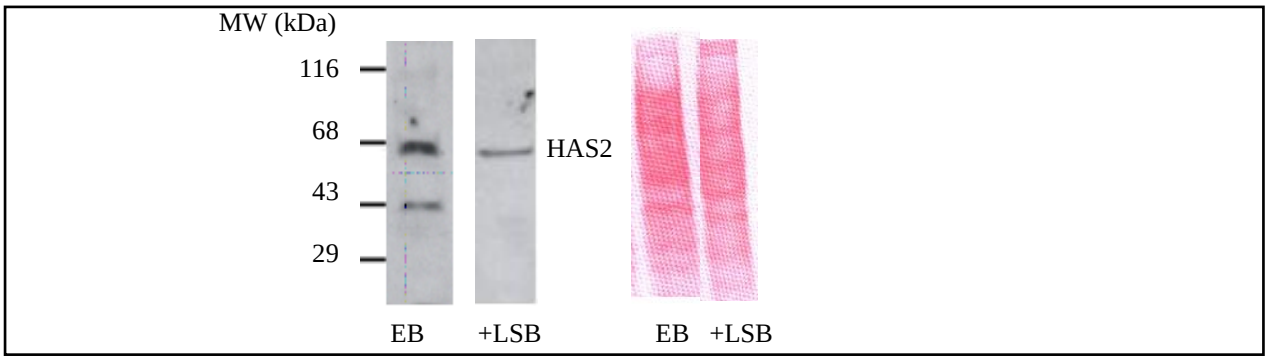

Figure 7) Un-stimulated HAS2 protein expression in HUVEC. *HUVEC were cultured in no-shear stress conditions for 24 h and extracted with either extraction buffer (EB) or they were directly extracted into 5 x Laemmli sample buffer (+ LSB). Analysis for HAS2 was done by immunoblotting. The corresponding Ponceau staining is shown in the right panel as a loading control.*

For validation of HAS2 immunoblotting in HUVEC, 3T3 fibroblasts were used as positive controls (data not shown). As immunoblotting showed two congenial regulated bands for HAS2, specificity of this effect was ensured by using specific blocking peptide. Both bands were blocked to a similar extent with the same specific blocking peptide in HUVEC and 3T3-

fibroblasts. Unspecific bands did not vanish after incubation with blocking peptide (data not shown).

As Laemmli sample buffer contains both sodium phosphate and 2 % SDS, it interferes with the Biorad protein assay according to Bradford. In order to stick to this protein assay because of the rapid procedure and its high sensitivity, the extraction buffer for protein extraction (see 2.1.1 and 2.2.6) was used in this work. Thus, the upper band represents the intact protein with a molecular weight matching to the molecular weight of HAS2 enzyme (EC 2.4.1.212) in human (63,566 Da) and the lower band a degradation product, together representing the overall amount of HAS2 in intact cells.

Immunofluorescence was used with two different HAS2 antibodies to show HAS2 protein distribution in un-stimulated HUVEC. Figure 8 shows a granular distribution HAS2 protein in different cells, neither with a cytoplasmatic accentuation or an accentuation of the core. Panel A and panel B show similar staining characteristics. As a negative control the second antibody was used only (panel C).

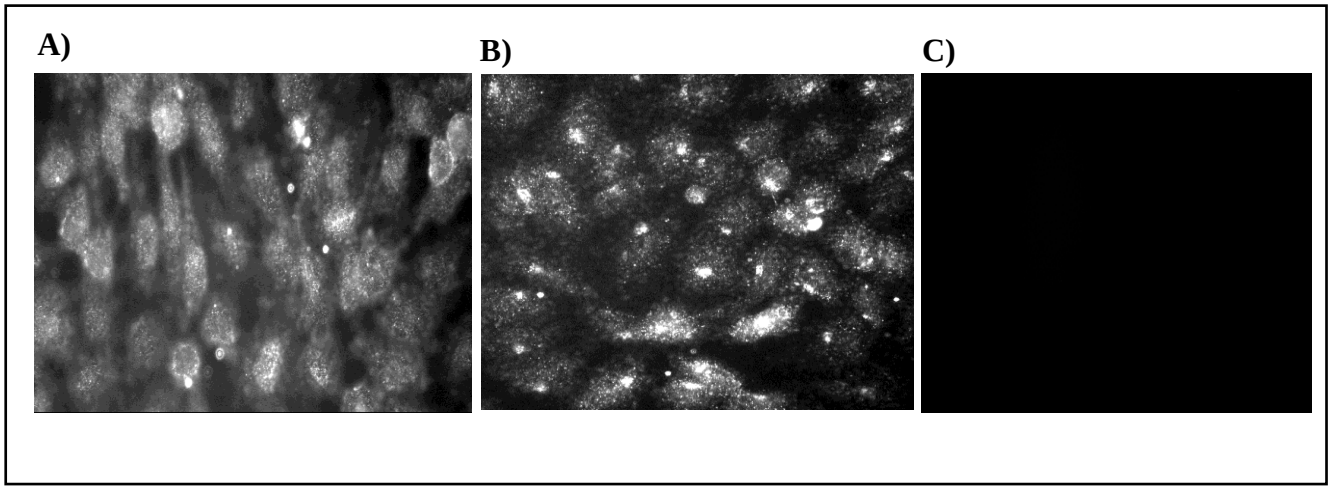

Figure 8) Expression of HAS2 in HUVEC analysed by immunofluorescence. *HUVEC were kept in no-shear stress conditions for 24 h and were then analysed by immunofluorescence using two different anti-HAS2 antibodies. Panel A) shows HAS2 expression in HUVEC using HAS2 antibody Sc-34067. Panel B) shows HAS2 expression in HUVEC using HAS2 antibody Sc-66916. Panel C) shows a representative negative control to panels A and B, using the respective secondary antibody only.*

3.2 Modulation of hyaluronan synthase 2 expression by constant shear stress

HUVEC, cultured in control conditions without shear stress, or stimulated with constant shear stress (6 dyn/cm²) for different periods of time were analysed for HAS2 expression (figure 9). HAS2 mRNA was analysed by rtq-RT-PCR, using GAPDH as a housekeeping gene (figure 9A), HAS2 protein expression was determined by immunoblotting (figure 9B and C). Endothelial HAS2 expression was induced in a transient and biphasic manner both on the mRNA and on the protein level each compared to the corresponding no-shear stress control. HAS2 mRNA increased from 2 h after the onset of flow onwards, reaching statistical significance after 4 h. A second, statistically not significant, increase was observed after 16 h of flow. With a somewhat later onset, but likewise reaching statistical significance, immunoblotting revealed two distinct maxima of HAS2 protein expression after 4 h and 16 h of stimulation with shear stress, and then decreased again.

The following experiments were done for 4 h, because the first significant peak expression of HAS2 was found after this time. When cells were exposed to different amounts of constant shear stress (2 dyn/cm² to 20 dyn/cm²), HAS2 mRNA and protein in HUVEC were expressed in a bell-shaped manner, with a statistically significant peak at 6 dyn/cm² (figure 10).

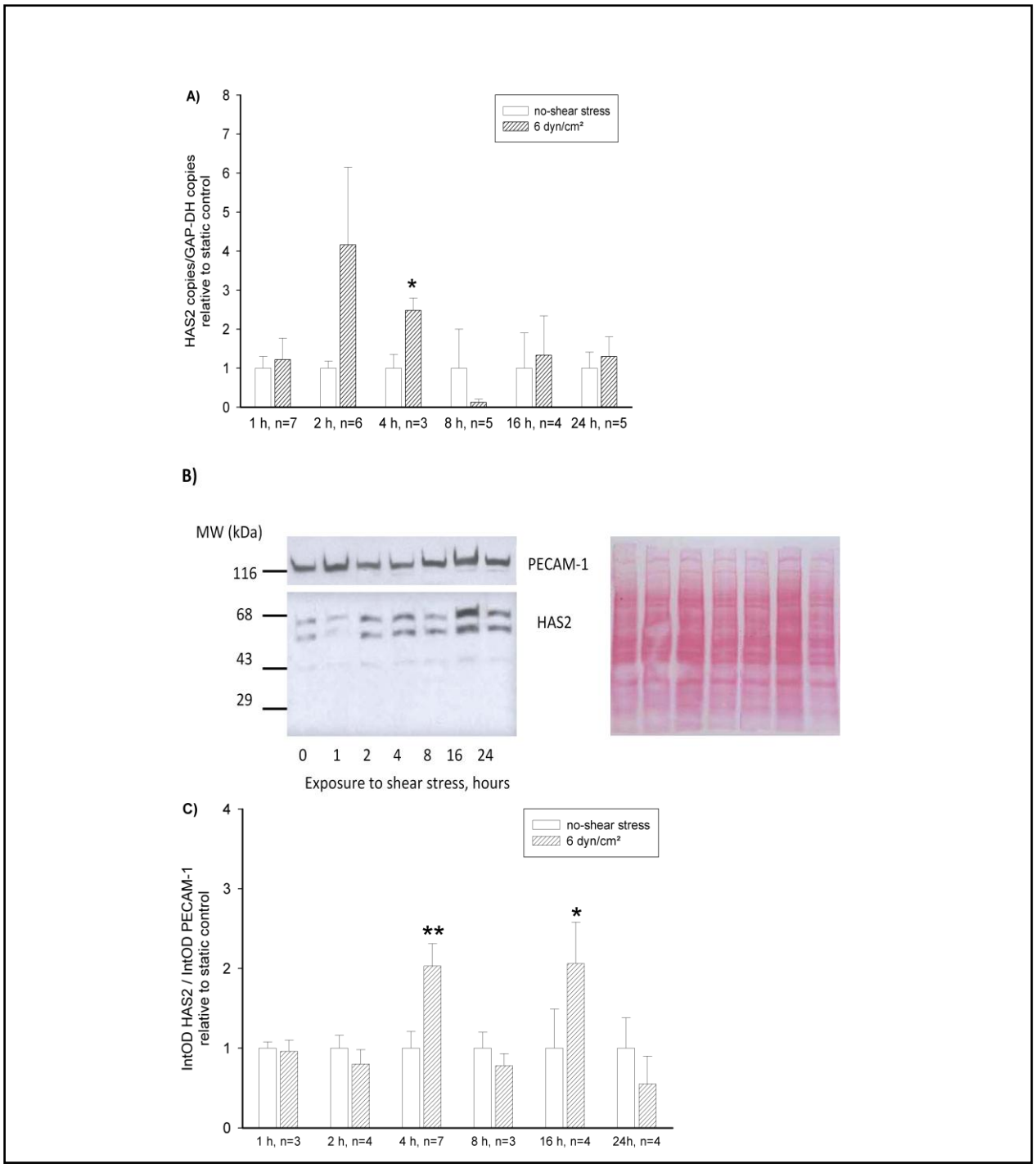

Figure 9) Time-dependent increase of HAS2 mRNA and protein through constant shear stress. *HUVEC, cultured in no-shear stress or constant shear stress conditions (6 dyn/cm²) for different time intervals (exposition time to shear stress from 1 h to 24 h) as indicated, were analysed by rtq-RT-PCR (A) and immunoblotting (B, C) for HAS2. B: Representative immunoblot of HAS2 using PECAM-1 and Ponceau staining (right panel) as loading control. Data are presented as means ± SEM of (n) independent paired samples. *p≤0.05, **p≤0.01.*

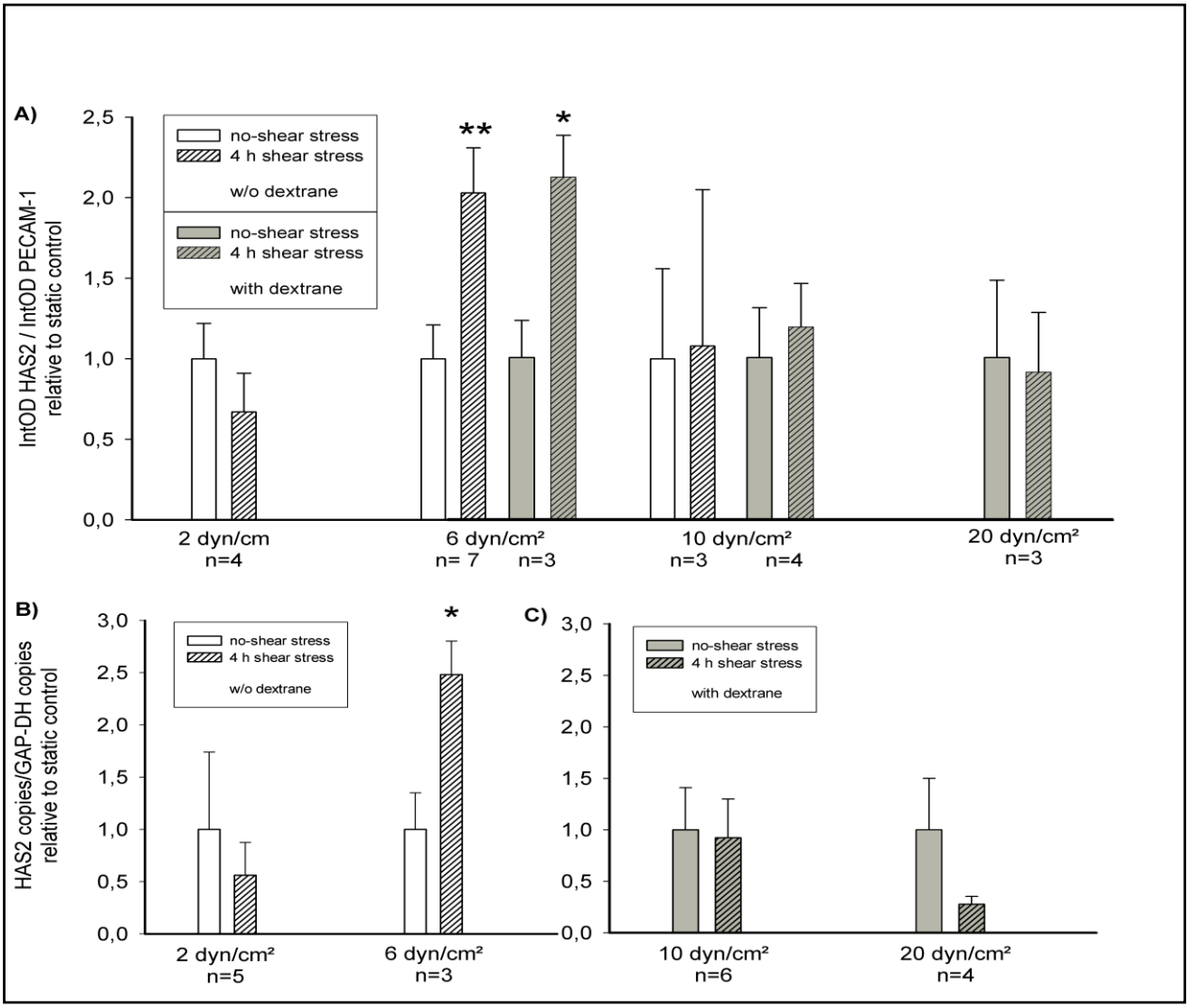

Figure 10) Force-dependent increase of HAS2 mRNA and protein through constant shear stress. *HUVEC, cultured in no-shear stress or constant shear stress conditions (2-20 dyn/cm², 4 h) in the absence (w/o dextrane) or presence (with dextrane) of dextrane, were analysed for HAS2 by immunoblotting (A) and rtq-RT-PCR (B, C). Data are presented as means ± SEM of (n) independent paired samples. *p≤0.05, **p≤0.01. Data at 6 dyn/cm² without the addition of dextrane were replotted from figure 1.*

To validate the specificity of the bell-shaped shear stress-dependent increase of HAS2, the same samples were analysed for ADAMTS1 and for eNOS (figure 11). ADAMTS1 protein expression increased from 10 dyn/cm² onwards. eNOS protein expression was increasingly up-regulated from 6 dyn/cm² up to at least 20 dyn/cm².

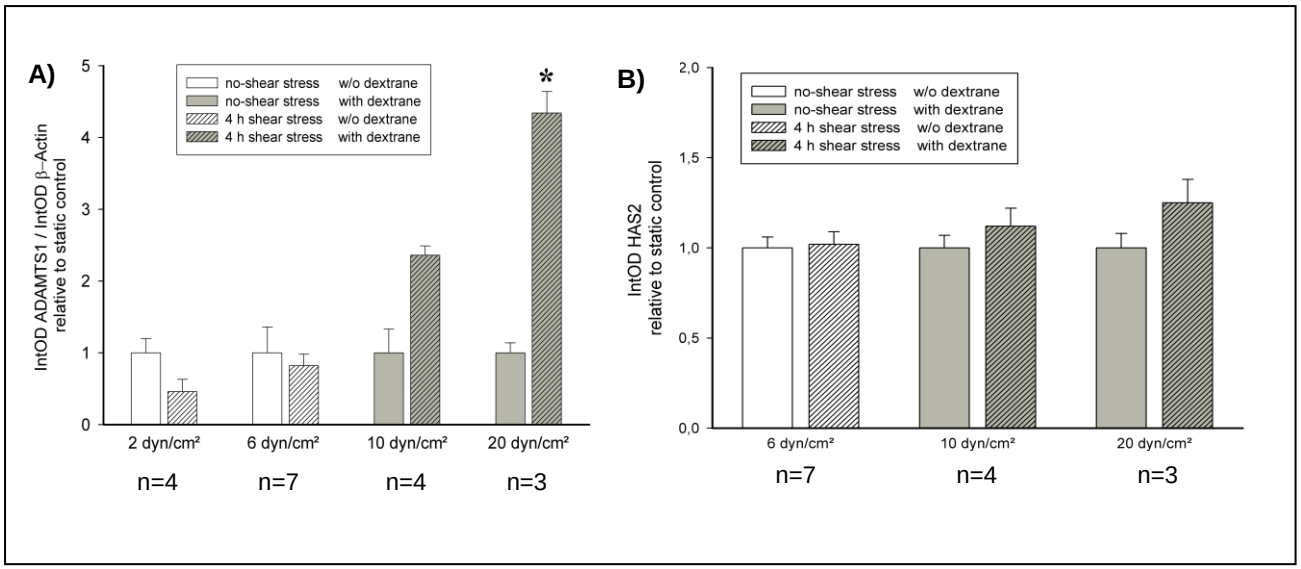

Figure 11) Force-dependent increase of ADAMTS1 and eNOS expression through constant shear stress. *HUVEC, cultured under no-shear stress or constant shear stress conditions (2-20 dyn/cm², 4 h), were analysed for ADAMTS1 protein expression (A) and for eNOS protein expression (B) by immunoblotting. Data are presented as means ± SEM of (n) independent paired samples. *p≤0.05, **p≤0.01.*

3.3 Effect of pulsatile flow on endothelial hyaluronan synthase 2

HUVEC were cultured for 24 h, either in control conditions without shear stress or they were stimulated with atheroprone, constant (6 dyn/cm²) or atheroprotective shear stress. After shear stress exposure HUVEC were analysed for HAS2 mRNA expression by rtq-PCR, using GAPDH as a housekeeping gene (figure 12). Atheroprotective flow revealed a statistically significant four-fold induction of HAS2 mRNA compared with no-shear stress control samples and with atheroprone shear stress. HAS2 mRNA was not changed above no-shear stress control levels under atheroprone flow conditions and its slight induction by constant laminar flow (6 dyn/cm², 24 h) did not reach statistical significance.

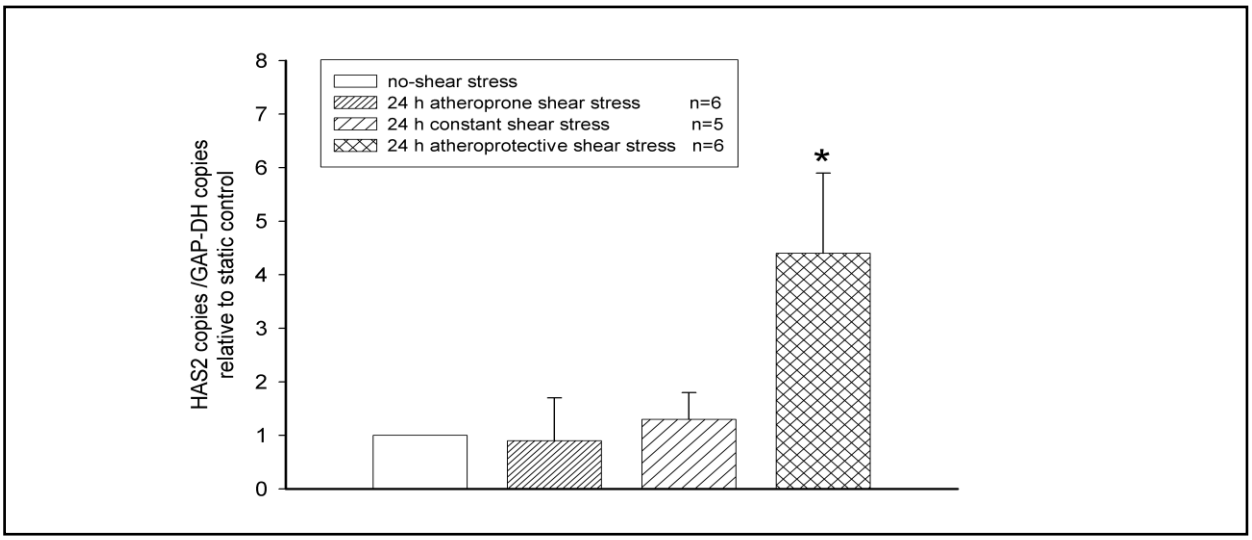

Figure 12) Increase of HAS2 mRNA through atheroprotective flow. *HUVEC, cultured in no-shear stress control conditions, exposed to "atheroprone", constant (6 dyn/cm²) or "atheroprotective" shear stress for 24* h*, were analysed by rtq-RT-PCR for HAS2 mRNA. Data are given as means ± SEM of (n) independent unpaired samples. *p≤0.05, both compared to no-shear stress control and to atheroprone samples.*

3.4 Effects of PI3K- and Akt-inhibition on endothelial hyaluronan synthase 2

To investigate whether mechanosensitive pathways play a role in shear-stress-induced expression of HAS2 mRNA and protein expression, HUVEC were cultured in control conditions without shear stress or were stimulated with constant shear stress (6 dyn/cm², 4 h) in the absence or presence of specific inhibitors of PI3K or Akt (figure 13 and 14). Inhibition of PI3K by LY 294,002 caused a nearly complete down-regulation of HAS2 mRNA below that of no-shear stress conditions. However, there was still a small, statistically not significant, shear-stress mediated induction of HAS2 mRNA expression detectable in the LY-treated samples. These results were supported by Western Blot analysis (figure 13), that revealed a complete and likewise statistically significant decrease of shear stress up-regulation.

Similarly, treatment with Akt-Inhibitor IV (AI) for 4 h showed a complete and statistically significant down-regulation of shear stress-induced HAS2 protein expression (figure 14).

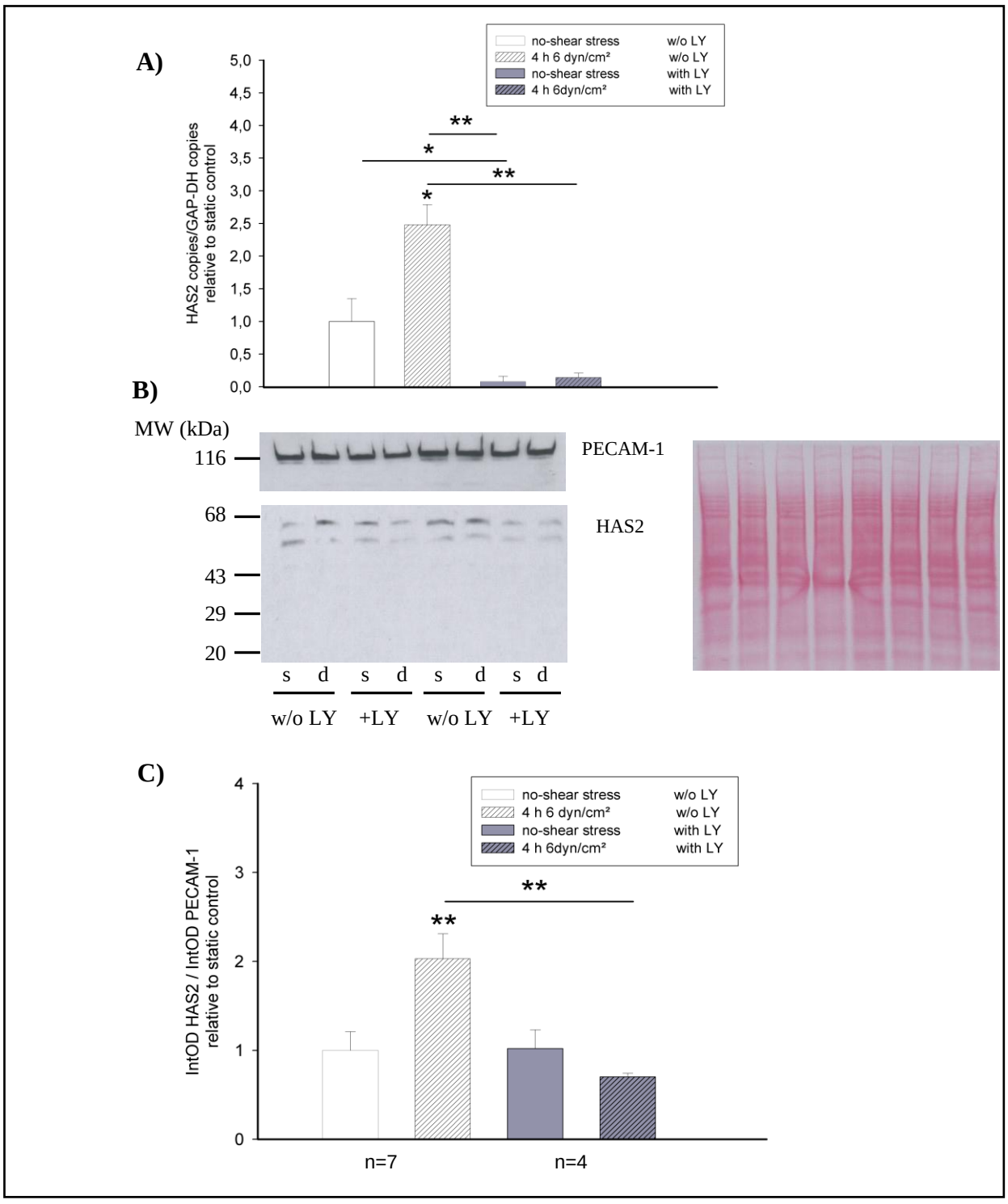

Figure 13) Inhibition of the shear stress-dependent increase of HAS2 by PI3K-Inhibitor LY 294,002. *HUVEC were cultured under no-shear stress or constant shear stress conditions (6 dyn/cm², 4 h) (w/o LY) or first treated with the PI3K-Inhibitor LY 294002 (+LY). (A): Analysis by rtq-RT-PCR of 3 independent paired samples.(B): Representative immunoblot of HAS2 with PECAM-1 as a loading control. The corresponding Ponceau staining is shown in the right panel as a loading control. (C): Densitometric analysis of immunoblotting of (n) independent unpaired samples. Data are given as means ± SEM. *p≤0.05,. **p≤0.01. Data at 6 dyn/cm² were replotted from figure 1.*

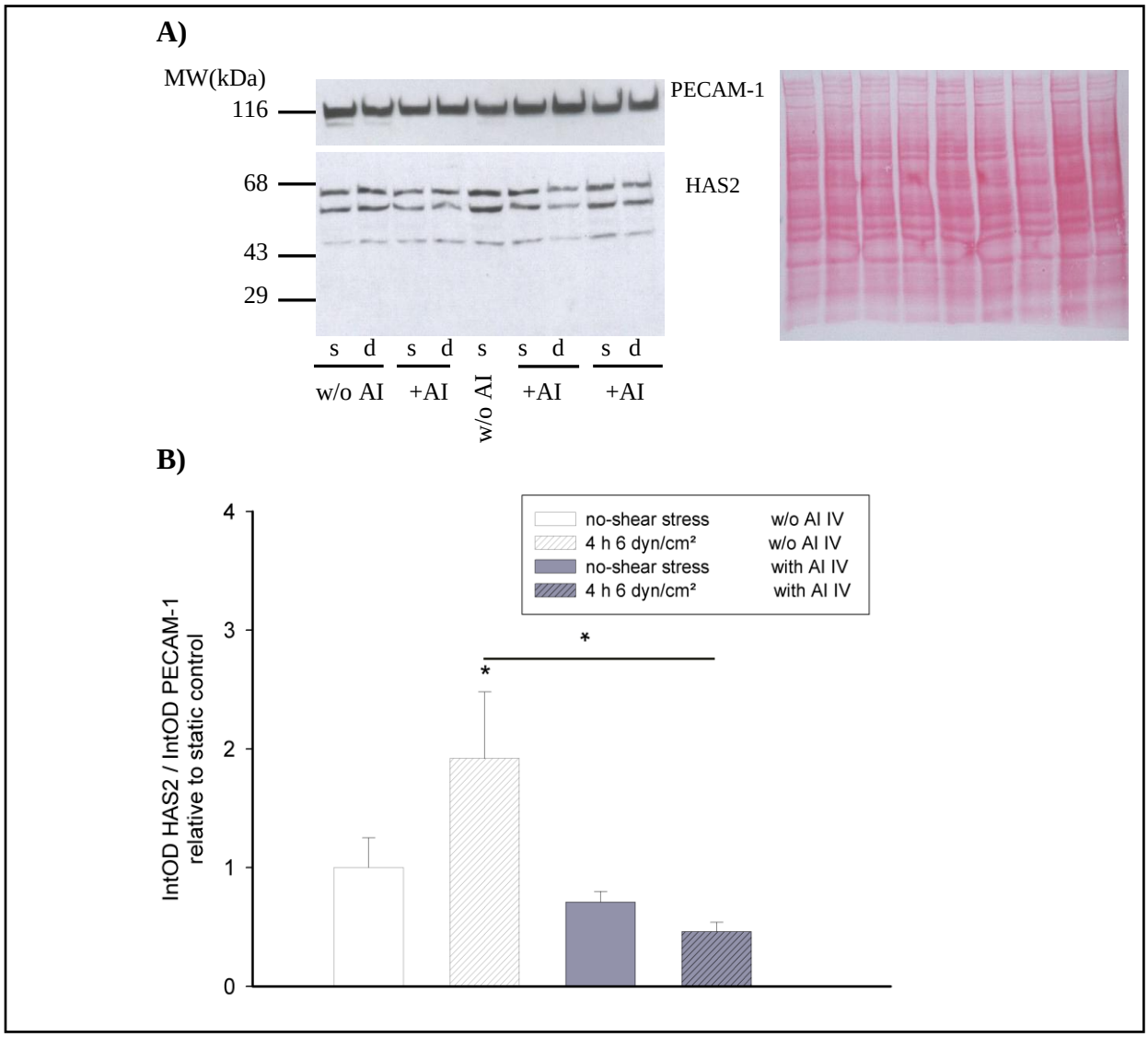

Figure 14) Inhibition of the shear stress-dependent increase of HAS2 by Akt-Inhibitor IV. *HUVEC, cultured in no-shear stress or constant shear stress conditions (6 dyn/cm², 4 h, w/o AI) or first treated with Akt-Inhibitor IV (+AI), were analysed by immunoblotting for HAS2. (A): Representative immunoblot of HAS2 with PECAM-1 as a loading control. The corresponding Ponceau staining is shown in the right panel as a loading control. (B): Data are given as means ± SEM of 3 independent paired samples. *p≤0.05. Data at 6 dyn/cm^2 were replotted from figure 1.*

3.5 Effect of constant and atheroprotective shear stress on endothelial hyaluronan

HUVEC, kept in control conditions without shear stress, or stimulated for 24 h with constant (6 dyn/cm²) or "atheroprotective" shear stress, were analysed with competitive ELISA for the hyaluronan concentration in the supernatant and the trypsinated fraction (ESL) (15) (figure 15). Supernatant from no-shear stress cells contained 3.85 ± 1.08 ng/ cell x 10^4 hyaluronan. While HA in the supernatant after stimulation with constant shear stress rose to 140%, stimulation with "atheroprotective" shear stress revealed an induction to about 400%. Hyaluronan in the trypsinated fraction of cells cultured in no-shear stress conditions amounted to 53 ± 25 ng/ cell x 10^4, only induced through "atheroprotective" shear stress to more than 150%. The total amount of HA of no-shear stress-cultured cells in supernatant plus ESL was about 57 ng/ cell x 10^4. 93 % of this amount were found in the trypsinated ESL fraction and only 7 % were found in the supernatant. After stimulation with pulsatile atheroprotective shear stress, 84% of the overall amount of HA (about 94.9 ng/ cell x 10^4) were found in the trypsinated fraction and 16% in the supernatant. The increase of the total amount of HA was about 38 ng/ cell x 10^4. Two-third of that were found in the trypsinated fraction and one-third in the supernatant. There was no observable effect of shear stress on the number of cells per culture dish [1.85 ± 0.26 x 10^6 versus 1.64 ± 0.35 x 10^6 cells/petri-dish, no-shear stress vs. shear stress, n=10].

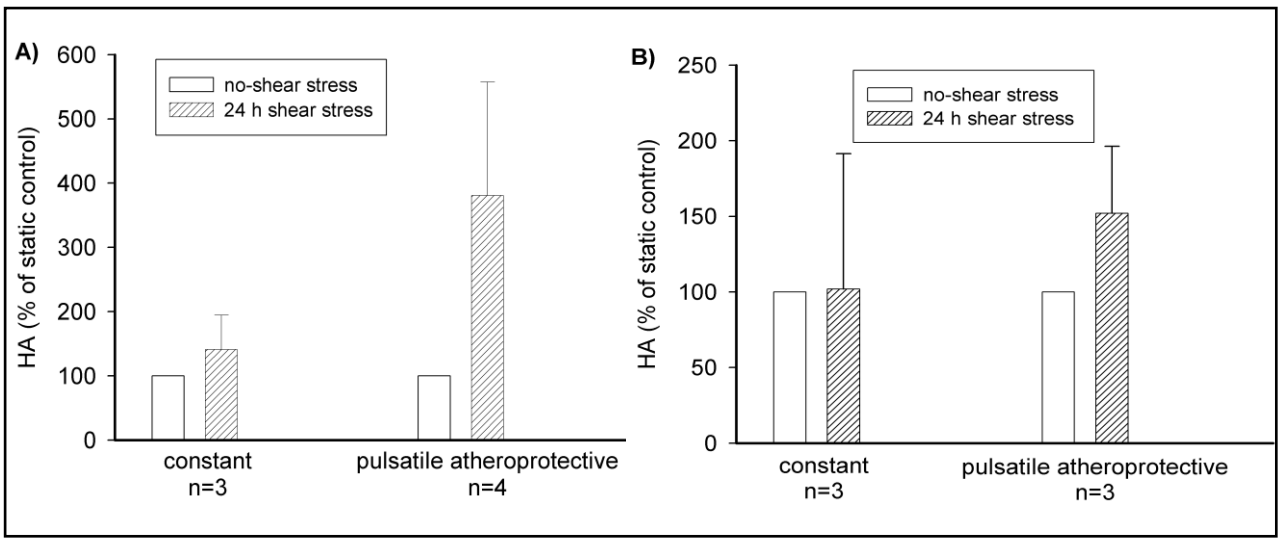

Figure 15) Increase of hyaluronan in supernatant and ESL through atheroprotective flow. *Data at 6 dyn/cm² were replotted from figure 1. HUVEC, kept under no-shear stress conditions, cultured with constant (6 dyn/cm²) or pulsatile "atheroprotective" shear stress (24 h), were analysed with competitive ELISA for hyaluronan in supernatant (A) and ESL (B). Data are presented as means ± SEM of (n) independent samples.*

3.6 Effects of PI3K-inhibition on hyaluronan in the ESL

To investigate whether mechanosensitive pathways play a role in the shear-stress dependent increase of HA, HUVEC were cultured for 24 h in control conditions without shear stress or were exposed to constant laminar shear stress (6 dyn/cm²) in the absence or presence of LY 294,002. After incubation, HUVEC were analysed by ELISA for HA concentration in the trypsinated fraction. Treating HUVEC with LY 294,002 (+10µmol/L) caused a statistically significant down-regulation of hyaluronan in the ESL of HUVEC exposed to constant laminar flow, as compared to untreated flow-exposed samples (figure 16). There was no statistically significant effect on the number of cells per petri dish [1.39 ± 0.23 x 10^6 versus 1.47 ± 0.37 x 10^6cells/Petri-dish, untreated cells vs. cells incubated with 10µmol/L LY, n=6 experiments].

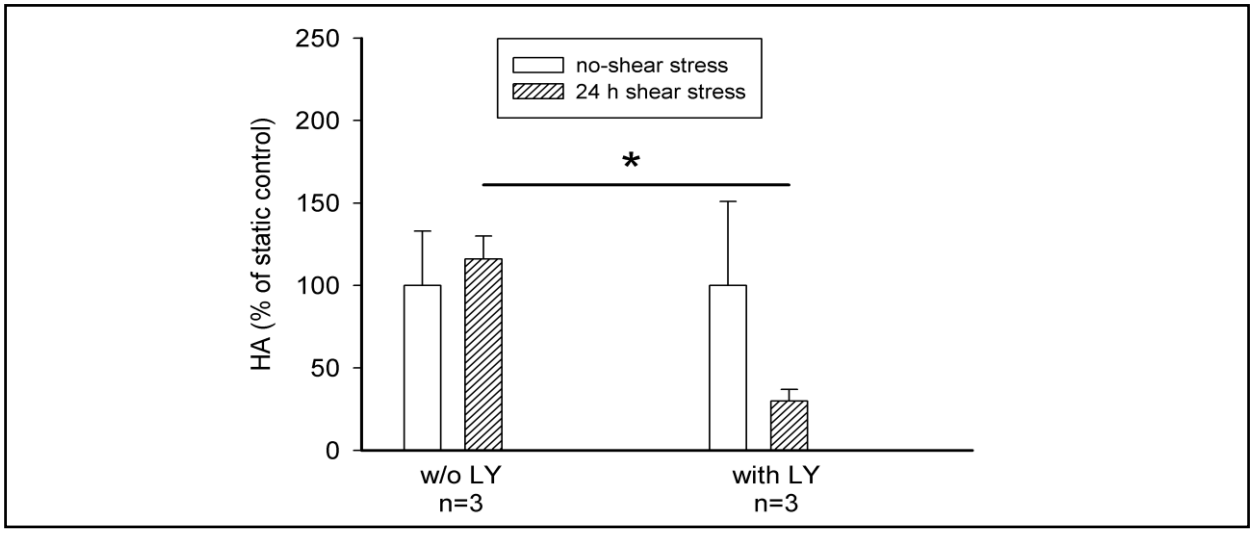

Figure 16) Decrease of hyaluronan in the ESL by PI3K-Inhibitor LY 294,002. *HUVEC were kept under no-shear stress conditions or were cultured with constant shear stress (6 dyn/cm², 24 h) either in the absence or presence of the PI3K-Inhibitor LY-294,002 as indicated. Analysis of hyaluronan in the trypsinated fraction (ESL) was performed using a competitive ELISA. Data are presented as means ± SEM of 3 independent paired samples.* p≤0.05, as compared to untreated flow-exposed samples.*

4 Discussion

4.1 Main results and possible interpretations

The present study demonstrates that hyaluronan synthase 2 and hyaluronan in endothelial cells are flow-dependently increased via the PI3-kinase-Akt-pathway with the most pronounced effect resulting from atheroprotective shear stress. Unstimulated endothelial cells express high amounts of HAS2 mRNA and protein. This expression can be significantly increased by distinct laminar constant and pulsatile shear stress. Particularly a normal arterial flow profile called "atheroprotective" considerably increases endothelial content of HAS2 mRNA synthesis as well as that of hyaluronan in ESL and supernatant. These findings confirm the central role of shear stress in endothelial cell biology and may provide a mechanism to regulate the thickness of the ESL in response to blood flow profiles. This cellular mechanism could help to understand the reduction of the ESL-dimension at sites with disturbed blood flow, as well as its increase at sites with laminar unidirectional blood flow, which has been previously observed *in vivo*. Thus, it may contribute to a better understanding of flow-dependent atheroprotective mechanisms (10).

4.2 Models for endothelial cells

HUVEC are widely used for experiments simulating arteriosclerosis prone conditions in humans *in vitro*, as well as for investigating the mechanotransduction induced by fluid dynamics (2, 3, 10, 15, 55). Thus, in the present study first passage human umbilical vein endothelial cells were used as a model for endothelial cells lining human vessels.

However, endothelial cells show large heterogeneity among and within tissues (9). Moreover, endothelial cells from diverse tissues are also heterogeneous with respect to their surface phenotype and protein expression. Some studies observed a greater responsiveness of human coronary artery endothelial cells (HCAEC) to pro-inflammatory stimuli than HUVEC and particularly microvascular endothelial cells (HMVEC) (24). However, HUVEC in this study, in passage four to six, still showed a strikingly greater responsiveness to inflammatory cytokines than HMVEC and only a slightly lesser one than HCAEC. In differential display studies, HUVEC showed a similarity in gene expression in response to shear stress, both to human

coronary microvascular endothelial cells (HCMEC) and to HCAEC (personal communication Dr. rer. nat. M. Bongrazio). This could mean that in general endothelial heterogeneity results from the respective environmental stimuli, most often because of distinct shear stress conditions, cytokines, plasma lipids and proteins (9).

In this study first passage cells were chosen to ensure that endothelial characteristics were not lost through de-differentiation during the number of passages. Furthermore, HUVEC used for experiments were not pooled. Thus, the number of experiments refers to the number of umbilical cords, reflecting biological differences between donors and deviations by the measurements as well.

Potter et al. (37) stated that the endothelial cell glycocalyx could not be observed in an *in vitro* experiment using HUVEC up to the ninth passage cultured under non-flow conditions (although tested with flow). By contrast, Vink et al. (15) and Pahakis et al. (35) used endothelial cells of lower passages and cultivated in shear stress-conditions for *in vitro* experiments investigating both the ESL structure and the ESL-dependent mechanotransduction of fluid shear stress. In the present work, HUVEC were chosen as a model for simulating atheroprotective and atheroprone conditions *in vitro*, and their effect on the synthesis of hyaluronan was investigated.

4.3 Hyaluronan synthase 2 expression in unstimulated endothelial cells

HUVEC cultured without flow express HAS2 mRNA, as this was shown so far only for microvascular endothelial cells by Suzuki et al. (44). The present study also shows the expression of HAS2 protein. Results were validated with a specific blocking peptide for immunoblotting and by comparing different methods of protein extraction. Rtq-PCR was validated by running non-RT controls. Thus, rtq-RT-PCR and immunoblotting detected HAS2 mRNA and -protein specifically.

In addition, endothelial HAS2 expression in un-stimulated HUVEC was visualised by immunofluorescence. A granular distribution of HAS2 protein, rather with an accentuation of the inner plasma membrane was visible, which would support the exceptional place of synthesis of hyaluronan at the inner face of the plasma membrane, in contrast to other GAG (1).

4.4 Application of constant and pulsatile flow

In order to discriminate between static and shear stress-conditions, HUVEC were exposed to constant shear stress. In arteries, blood flow is generally considered to be laminar (11) and accepted as being atheroprotective, while low flow that changes direction is considered to be atheroprone. A recent study showed average amounts of undisturbed shear stress *in vivo* ranging approximately between a mean shear stress of 4 and 16 dyn/cm² in the human a. carotis communis (10). In contrast, Chatzizisis et al. (7) assume higher amounts of undisturbed shear stress with a magnitude that varies within a range of 15 to 70 dyn/cm². Thus, to investigate a force dependent regulation of HAS2, and to account for different *in vivo* conditions, shear stress was changed between 2 and 20 dyn/cm².

In vivo, because of the pumping heart, shear stress occurs most often as a pulsatile profile. Pulsatility is observed not only in larger proximal arteries, but even down to arteriolar, capillary and even venular vessels in the microcirculation (17, 29). At vascular sites with low risk for arteriosclerosis, shear stress of more than 40 dyn/cm² can be reached occasionally (10). At these sites shear stress appears most often as a pulsatile pattern with unidirectional flow and higher rates of acceleration, but shows also different amounts of peak and mean shear stress (7, 10, 11, 47).

In contrast, shear stress at vessel sites which are prone to arteriosclerotic plaque formation, such as the vicinity of branch points, the outer wall of bifurcations and the inner wall of curvatures (11, 47) display a larger heterogeneity. Here, vessel geometry promotes flow separation and turbulences generating disturbed shear stress. Thus, shear stress fluctuates greatly in pressure and magnitude over short distances, resulting in very low time-average shear stress, usually close to zero (7). These shear stress patterns are characterised by less intensive acceleration and deceleration when compared with undisturbed flow, but exhibiting directional changes of shear stress and even reverse flow (10).

A cone-and-plate-system with a small DC motor was used simulating constant laminar flow with different shear stress. The application of higher pulsatile laminar and bidirectional flow required the construction of a cone-and-plate-device, with less inertia and a much stronger motor. In

addition, because of the complexity of the applied flow profiles, a computer interface with a special software programme became necessary to simulate the shear stress waveforms.

In summary, the distinct constant and pulsatile shear stress-conditions, which were applied to HUVEC in the present study do account for various different shear stress conditions found *in vivo* at different vessel sites.

4.5 Shear stress-dependent endothelial hyaluronan synthase 2 expression

4.5.1 Time-course

Constant laminar flow generating shear stress of 6 dyn/cm² proved to increase a transient time-dependent synthesis of endothelial HAS2, on both the mRNA and protein level with two distinct peaks of HAS2 protein expression. The induction of endothelial HAS2 expression could result from at least two different pathways of cellular signal transduction being involved in HAS2 expression regulation. Moreover, a relatively rapid increase/decrease of the HAS2 protein concentration might indicate a fast turnover rate. The results were verified, analysing GAPDH expression on mRNA level and PECAM-1 expression on protein level in the same samples. Both genes were continuously expressed in HUVEC, independent of the application of shear stress (43).

Many endothelial genes have been found to be shear stress-dependently regulated, particularly considering time dependent effects (2, 3, 4, 8, 10, 28, 43). In previous studies mechanotransduction of shear stress to endothelial cells was investigated especially for the first couple of hours of shear stress exposure (4, 28, 42). Biomechanical responses to shear stress are very heterogeneous: Thus, some second messengers like inositol 1,4,5 trisphosphate (IP3) and diacylglycerol (DAG) are activated within seconds, while cytoskeletal changes, VCAM-1 down-regulation and connexin 43 up-regulation are achieved in a couple of 1-8 h (4). Moreover, long lasting effects were found, which could play an important role particularly for structural vessel adaptation which was investigated with special regard to angiogenesis (2, 3). Several genes were progressively down-regulated after long-time exposure to shear stress (up to 48 h), e.g. angiopoetin-2 (8). Others were increased to a maximum already after only 4 h of shear stress exposure, in order to sustain over the time up to 48 h, e.g. METH-1 or ADAMTS1 (18).

Furthermore, some genes were up-regulated only after prolonged exposure to shear stress (24-48 h), e.g. gas-3 (2, 8). In addition, there were transient time-dependent effects described for a couple of genes comparable to the observed effects on HAS2 reported here. Foxo-1 (8) was down-regulated after shear stress exposure with a maximum after only 4 h and a following increase but still lower expression than control after 24 h of shear stress exposure. Tissue factor was induced after 4 h of shear stress application and subsequently reduced to basal expression after 12 h (28). Monocyte chemotactic protein-1 was induced in a biphasic manner, with peaks after 1.5 h and 2.5 h of stimulation with constant shear stress of 6 to 32 dyn/cm² (43).

To conclude, various transient effects of shear stress on endothelial gene expression may support the observations for HAS2 in this study. However, in contrast to HAS2 protein, the HAS2 mRNA was significantly up-regulated only after 4 h. In order to explain these observations, further studies will be necessary to investigate the span in between 4 and 16 h in detail.

4.5.2 Force dependency

Varying shear stress between 2 dyn/cm² and 20 dyn/cm², a bell-shaped function of HAS2 with a peak at 6 dyn/cm² was found. To validate this unexpected observation, ADAMTS1 and eNOS were tested in the same samples and were found to increase continuously with increasing shear stress up to at least 20 dyn/cm². Thus, the bell-shaped increase of endothelial HAS2 appeared to be specific.

With respect to the literature, higher/lower constant laminar flow was observed to increase or decrease endothelial gene expression, respectively (3, 4, 8, 22, 46). Especially eNOS was described to be induced after application of high mean constant shear stress, having vaso-dilatational and atheroprotective effects (22). Other genes were decreased after the application of higher amounts of shear stress, e.g. angiopoetin-2 (8). However, at least one study showed a similar peak increase of PDGFβ at a shear stress of 6 dyn/cm^2 (19), although this was not discussed in the manuscript.

According to the average amounts of undisturbed shear stress *in vivo* as discussed above, the shear stress-dependent expression of endothelial HAS2 reported here may maximize its *in vivo* availability under normal flow conditions. However, great care must be taken in extrapolating *in*

vitro data into *in vivo* physiology. The bell-shaped endothelial HAS2 expression might have different peak-values *in vivo* or in different species.

4.5.3 Pulsatile waveforms

The atheroprotective shear stress profile was proven to be an even stronger stimulus for an increase of endothelial HAS2 expression *in vitro* than constant laminar flow. This may indicate a special role of endothelial HAS2 in protection against arteriosclerosis.

Endothelial HAS2 expression was considerably lower after the stimulation with atheroprone flow, found at vascular sites with assumed small ESL. Lower HAS2 expression possibly explains reduced ESL-dimensions at vascular sites with disturbed flow *in vitro*, while an increase in endothelial HAS2 expression after the stimulation with an atheroprotective flow profile may assist shear stress-dependent incorporation of HA into the ESL (15).

As flow conditions are heterogeneous at different vascular sites, further studies are necessary to investigate pulsatile flow patterns and their effects on endothelial HAS2 expression in detail.

4.5.4 Intracellular transduction pathways

Complete inhibition of shear stress-mediated induction of HAS2 mRNA and protein by either LY294,002 or Akt-inhibitor indicates the relevance of the PI3K/Akt-pathway in endothelial HAS2 regulation, at least for the rapid induction of HAS2 mRNA and protein expression after 2 to 4 h following the onset of shear stress.

Several signal transduction pathways are well known to be activated by shear stress acting on endothelial cells (26, 27, 36, 47). Shear stress could either act directly on the luminal endothelial cell surface via the ESL (13, 40) or be mechanically transmitted through the cell and activate cell-cell contacts or focal adhesion sites (42). PI3K is an early part of activated signalling pathways in all of these cases and therefore an important part in shear stress-mediated mechanotransduction (12, 30). One downstream target of the PI3K is Akt (PKB) which is also regulated by shear stress (14). Hence, complete inhibition of shear stress-induced up-regulation

of HAS2 mRNA and protein by blocking of Akt hence suggests a biological significance of the PI3K/Akt-pathway in endothelial HAS2 regulation. However, the present study did not test the relevance of the PI3K/Akt-pathway for the second induction of HAS2 at about 16 h. This second/delayed increase could be initiated through additional mechanotransduction pathways.

4.6 Future prospects

In this study, attention was drawn to endothelial HA synthases isoform 2. Of the three isoenzymes, HAS2 synthesizes extremely long HA chains with an high average molecular weight. Nevertheless all three isoforms were found in endothelial cells (44). Thus, in future studies the expression of all three enzymes should be approved and investigated in regard to different shear stress conditions, signal transduction pathways and different pro-arteriosclerotic conditions.

4.7 Hyaluronan in the ESL: Regulation through shear stress

The atheroprotective shear stress profile increased the amount of endothelial-derived HA in this study. This supports and even expands recent studies (15) that certain non-pulsatile shear stress conditions could stimulate the incorporation of HA into the ESL.

According to post-mortem anatomical studies, early arteriosclerotic lesions are preferentially located at vessel sites with disturbed blood flow like the vicinity of branch points, the outer wall of bifurcations and the inner wall of curvatures (4, 53). Studies were done that demonstrated a considerably thicker endothelial surface layer at regions with low risk for arteriosclerosis than at arteriosclerosis-prone sites with disturbed flow (48). Consequently, among others, hyaluronan incorporation at these arteriosclerotic resistant sites seems to be important for the thickness of the ESL. It has been assumed that dysfunction of the ESL is the first step for the initiation and progression of the arteriosclerotic process (34, 39).

Blocking of PI3K significantly reduced shear stress-stimulated HA in the ESL. However, this reduction was greater than the shear stress-dependent induction of HA content observed in the

ESL. This indicates a shift into the supernatant which cannot be compensated for by an increased production while PI3K is inactivated.

4.8 Expanding the picture of the endothelial surface layer

The molecular structure of HA is important for the size and the structure of the unimpaired ESL (31, 50). While heparan sulfate and chondroitin sulfate, which are next to hyaluronan the most important GAG in the ESL, have an average molecular weight of about 30 kDa (45, 52), HA has a molecular weight of up to 10^4 kDa with a corresponding length of a couple of micrometers. Local ionic strength and pH influence the level of extensibility of a GAG chain (52). In a physiological sodium chloride solution the extensibility seems to reach its maximum, so that GAG are considered to extend to approximately 80% of their contour length (41). Thus, especially the long disaccharide chain of HA weaves into the ESL (45) and may support the size of the ESL. Consequently, van den Berg et al. (50) observed a hairy-like structure in normal myocardial rat capillaries (figure 2, panel A). The thesis of long weaving disaccharide chains is indirectly supported by Secomb et al. (40). This group suggests from their theoretical analyses that the ESL consists of a matrix of molecular chains extending from the cell surface and being held in tension by slight increases in colloid osmotic pressure relative to that in free-flowing plasma (figure 16, panel A). The layer resists flattening as a result of colloid osmotic pressure generated by plasma proteins adsorbed to the ESL (38, 40). In contrast to a model with extending molecular chains from the plasma membrane, Tarbell et al. (45) and Weinbaum et at. (52) draw a picture of a more meshlike-structured ESL. In this model the long disaccharide chain of HA is connected to the ESL and lies on the endothelial plasma membrane, being bound to CD 44 (figure 16, panel B).

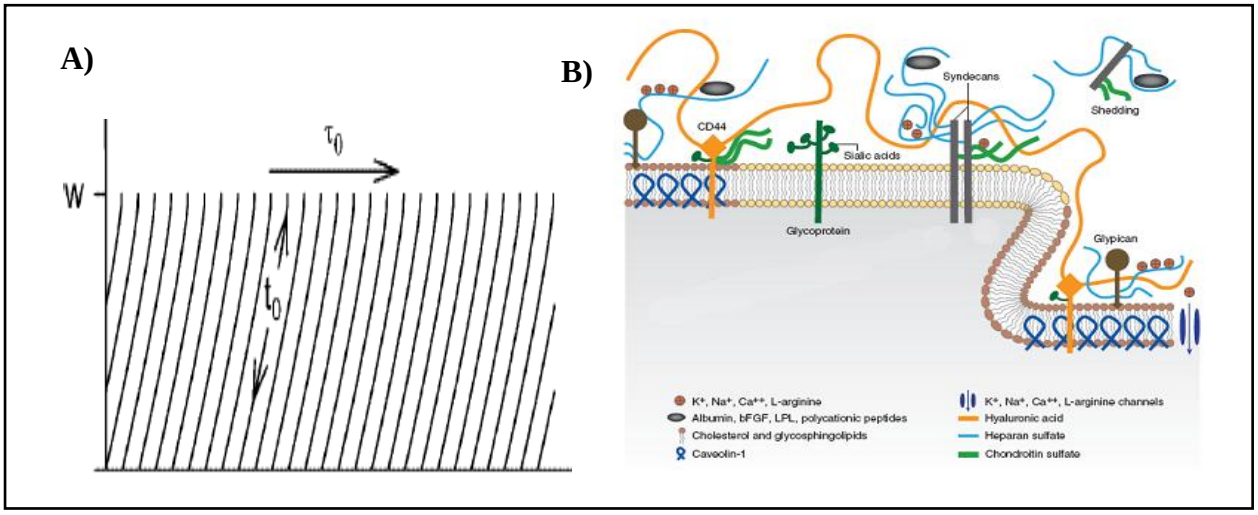

Figure 17) ***Two different models for the ESL.*** *Panel A shows the illustration of the ESL drawn by Secomb et al. (39) from a theoretical analysis: A matrix of strands is attached to the endothelial cell membrane and extends a distance w to the luminal site. These membrane-bound chain structures form the ESL (37). τ represents the fluid shear stress which is transmitted to the plasma membrane by tension (t_0). Panel B shows the model of the ESL illustrated by Tarbell et al. (44). Here, the components of the ESL are drawn in respect to their ratio in this layer and the ESL is seen more as a mesh-like surface structure.*

However, Pries (38) and Secomb et al. (40) suggest that the size of the ESL of at least 0.5 µm to 1.0 µm thick, is mainly achieved by interaction (a balance between adsorption and shedding) of soluble plasma components with a small membrane-bound glycocalyx. Other groups, i.e. Weinbaum et al. (52), favour an interaction of adsorption, shedding of ESL components into the flowing blood, and local synthesis of GAG by endothelial cells (15, 38, 39, 52).

Figure 18 was drawn in order to consider these different aspects and the special role of pulsatile flow for endothelial HAS2 and the incorporation of HA into the ESL. It provides a possible link between blood flow-generated shear stress, endothelial HAS2 expression and the amount of HA in the ESL, taking into account both the theoretical analysis of Secomb et al. (40) and the observation of a hairy-like structure covering the endothelium (50). Furthermore, this model tries to show the size of the ESL and the endothelium in relation to red blood cells, both at sites with arterial-like blood flow (panel B) as well as sites with disturbed blood flow (panel A). A couple of GAG attachments were omitted in this model for the sake of clarity of the illustration.

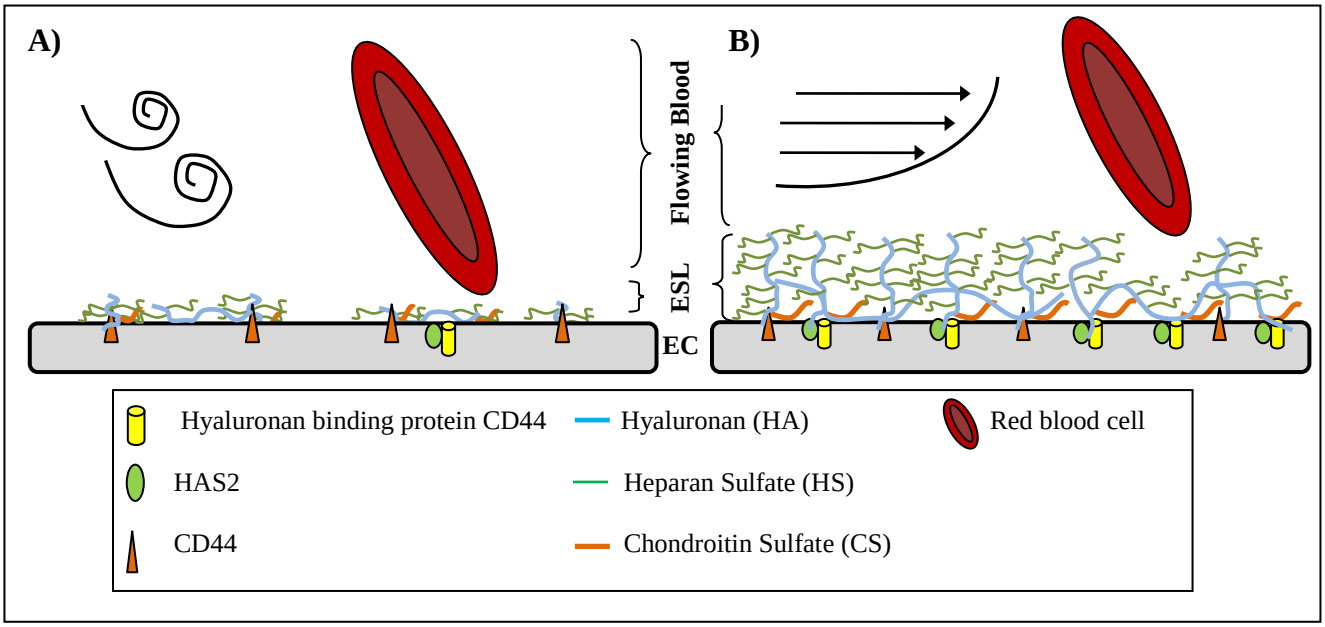

Figure 18) ***The ESL at vessel sites with disturbed or undisturbed blood flow.*** *Picture of glycosaminoglycans (GAG) in the ESL and hyaluronan synthase 2 (HAS2) in endothelial cells (EC) at sites with disturbed ("atheroprone") blood flow (panel A) and undisturbed ("atheroprotective") blood flow (panel B). The endothelial amounts of HAS2 under these different flow conditions were taken into consideration, represented in the number of molecules in the respective panel. Moreover, the illustration tries to account for the size of the ESL in respect to the endothelium and red blood cells. A couple of GAG attachments were omitted in this illustration. HA is associated to CD44 and to the plasma membrane-bound HAS2. The HA chain weaves into the ESL; HS and CS chains are attached to CD44 and HA, respectively.*

4.9 Summary and Conclusions

In summary, the present study shows the expression of HAS2 mRNA and protein in endothelial cells. It provides evidence for the hitherto unknown shear stress-induced content of endothelial HAS2 mRNA and protein expression via the PI3-kinase-Akt-pathway with special regard to an arterial-like flow profile. It proves the thesis of a shear stress-stimulated endothelial HA synthesis and its incorporation into the ESL. Additionally, it provides new evidence that especially an atheroprotective flow profile enhances endothelial HA synthesis. Furthermore, the results of the present work are combined with data of other studies, in order to re-draw the picture of the ESL and to provide a link between flowing blood generating atheroprotective shear stress, endothelial HAS2 expression and ESL structure. Thus, this work may stimulate further investigations into the role of the different HAS isoforms and of HA in the ESL, as an aegis (45) against the development of arteriosclerosis.

5 Abstract

Hyaluronan (HA), a highly negatively charged unsulfated glycosaminoglycan (GAG), with an extended length of up to 25 µm seems to be a constitutive component of the endothelial surface layer (ESL). It has been shown that the inner blood vessel surface is lined with a gel-like surface structure, measuring at least 0.5 µm thick. This layer is a protection against coagulation and inflammation, and defends the vessel wall from the development of arteriosclerotic plaques. Interestingly, the size of this surface layer is significantly reduced at vessel sites with disturbed blood flow and low shear stress. Removal of hyaluronan by treatment with hyaluronidase results in a reduction of the ESL to less than 0.1 µm thick and impaired vessel dilatation properties. Recently, studies showed that distinct shear stress conditions can increase the incorporation of hyaluronan into the ESL. Therefore, the present study was undertaken to prove the hypothesis that shear stress can increase the amount of endothelial hyaluronan synthase 2 (HAS2) *in vitro* and subsequently influence endothelial hyaluronan synthesis. Especially the effect of undisturbed, arterial-like pulsatile shear stress on endothelial HAS2 and hyaluronan synthesis was investigated. Human umbilical vein endothelial cells (HUVEC) were exposed to constant or pulsatile shear stress in a cone-and-plate system, in the absence or presence of specific inhibitors of phosphatidylinositol 3-kinase (PI3K) and Akt. Cells were analysed for HAS2 expression by real-time RT-PCR, by immunoblotting and by immunofluorescence. Analysis for hyaluronan concentration in the supernatant and the ESL was done by ELISA. HAS2 mRNA and protein, were found to be shear stress-dependently increased via the PI3K-Akt-pathway in a transient manner. Moderate constant shear stress of 6 dyn/cm² increased the endothelial HAS2 expression. Pulsatile, arterial-like shear stress conditions induced the enzyme and also endothelial-derived hyaluronan even more effectively. In contrast, lower shear stress and shear stress that continuously changed its direction did not induce any differences in comparison with control cultures not exposed to shear stress. These experiments provide evidence for the hitherto unknown shear stress-induced content of endothelial HAS2 via the PI3-kinase-Akt-pathway and prove the thesis of a shear stress stimulated endothelial hyaluronan synthesis and an increased incorporation of hyaluronan into the ESL, especially after stimulation with undisturbed arterial-like shear stress. Thus, the study provides a new link between the production of a constitutive component of the endothelial surface layer by endothelial cells and blood flow.

6 Index of abbreviations

ADAMTS1	A desintegrine and metalloprotease with thrombospondin-1 repeats
AI	Akt-Inhibitor IV
Akt	RAC-alpha serine/threonine-protein kinase
APS	Ammoniumperoxydisulphate
BP	Blocking peptide
BSA	Bovine serum albumin
CD	Cluster of differentiation
cDNA	Complementary deoxyribonucleic acid
CS	Chondroitin Sulphate
DAG	Diacylglycerol
DC	Direct current
DEPC	Diethyl cyanophosphonate
DMSO	Dimethylsulfoxide
dNTP	Deoxynucleotide
DTT	Dithiotreitol
EB	Extraction buffer
EDTA	Ethylendiamintetra acetic acid
ELISA	Enzyme-linked immunosorbent assay
eNOS	Endothelial cell nitric oxide synthase
ESL	Endothelial Surface Layer
Foxo-1	Forkhead box protein O1
GAG	Glycosaminoglycane
GAP-DH	Glyceraldehyde 3-phosphate dehydrogenase
GlcA	Glucuronic acid
GlcNAc	N-acetylglucosamine
HA	Hyaluronan
HAS	Hyaluronan synthase
HBSS	Hank´s balanced salt solution
HCAEC	Human coronary artery endothelial cells

HCMEC	Human coronary microvascular endothelial cells
HMVEC	Human microvascular endothelial cells
HS	Heparan sulphate
HUVEC	Human umbilical vein endothelial cells
IP3	inositol 1,4,5 trisphosphate
LSB	Laemmli sample buffer
MAP	Mitogen-activated protein
METH-1	Metalloprotease and thrombospondin1
MRI	Magnet resonance imaging
mRNA	Messenger ribonucleic acid
MW	Molecular weight
NO	Nitric oxide
PBS	Phosphate Buffered Saline
PDGFβ	Platelet derived growth factor β
PCR	Polymerase chain reaction
PECAM-1	Platelet endothelial cell adhesion molecule
PI3K	Phosphatidylinositol 3-kinase
PLC	Phospholipase C
PKC	Protein kinase C
rt-PCR	Reverse transcription PCR
rtq-PCR	Real-time quantitative PCR
SDS-PAGE	Sodium-dodecyl-sulfate polyacrylamide gel-electrophoresis
TBE	Tris/Borate/EDTA-Buffer
TEMED	Tetramethylethylenediamine
UDP	Uridine diphosphate
VCAM-1	Vascular cell adhesion molecule-1

7 Index of figures and tables

Figure 1: Scheme of distinct hyaluronan chain lengths and multiple functions of the three isoforms of hyaluronan synthases.
Figure 2: The ESL: Electron microscopy pictures of myocardial rat capillaries.
Figure 3: Shear stress patterns of constant and pulsatile laminar shear stress waveforms.
Figure 4: General outline of the cone-and-plate-system to simulate pulsatile flow.
Figure 5: Reproduction of flow patterns with the second cone-and-plate-device.
Figure 6: Cell shape and alignment after exposure to pulsatile shear stress profiles.
Figure 7: Un-stimulated HAS2 protein expression in HUVEC.
Figure 8: Expression of HAS2 in HUVEC analysed by immunofluorescence.
Figure 9: Time-dependent increase of HAS2 mRNA and protein through constant shear stress.
Figure 10: Force-dependent increase of HAS2 mRNA and protein through constant shear stress.
Figure 11: Force-dependent increase of ADAMTS1 and eNOS expression through constant shear stress.
Figure 12: Increase of HAS2 mRNA through atheroprotective flow.
Figure 13: Inhibition of the shear stress-dependent increase of HAS2 by PI3K-Inhibitor LY 294,002.
Figure 14: Inhibition of the shear stress-dependent increase of HAS2 by Akt-Inhibitor IV.
Figure 15: Increase of hyaluronan in supernatant and ESL through atheroprotective flow.
Figure 16: Decrease of hyaluronan in the ESL by PI3K-Inhibitor LY 294,002.
Figure 17: Two different models for the ESL.
Figure 18: The ESL at vessel sites with disturbed or undisturbed blood flow.

Table 1: Primers taken to produce template-cDNA.
Table 2: Primers taken for real-time quantitative PCR.

8 References

1 Allison DD, Grande-Allen KJ. Review. Hyaluronan: a powerful tissue engineering tool. Tissue Eng. 2006 Aug;12(8):2131-2140.

2 Bongrazio M, Baumann C, Zakrzewicz A, Pries AR, Gaehtgens P. Evidence for modulation of genes involved in vascular adaptation by prolonged exposure of endothelial cells to shear stress. Cardiovasc Res. 2000 Aug;47(2):384-393.

3 Bongrazio M, Da Silva-Azevedo L, Bergmann EC, Baum O, Hinz B, Pries AR, Zakrzewicz A. Shear stress modulates the expression of thrombospondin-1 and CD36 in endothelial cells in vitro and during shear stress-induced angiogenesis in vivo. Int J Immunopathol Pharmacol. 2006 Jan-Mar;19(1):35-48.

4 Braddock M, Schwachtgen JL, Houston P, Dickson MC, Lee MJ, Campbell CJ. Fluid Shear Stress Modulation of Gene Expression in Endothelial Cells. News Physiol Sci. 1998 Oct;13:241-246.

5 Bradford MM. A rapid and sensitive method for the quantitation of microgram quantities of protein utilizing the principle of protein-dye binding. Anal Biochem. 1976 May 7;72:248-54.

6 Bussolari SR, Dewey CF Jr., Gimbrone MA Jr.. Apparatus for subjecting living cells to fluid shear stress. Rev Sci Instrum.1982 Dec (53)12: 1851-4

7 Chatzisis YS, Coskun AU, Jonas M, Edelman ER, Feldman CL, Stone PH. Role of Endothelial Shear Stress in the Natural History of Coronary Atherosclerosis and Vascular Remodeling. J Am Coll Cardiol. 2007 Jun 26;49(25):2379-2393.

8 Chlench S, Mecha Disassa N, Hohberg M, Hoffmann C, Pohlkamp T, Beyer G et al.. Regulation of Foxo-1 and the angiopoietin-2/Tie2 system by shear stress. FEBS Lett. 2007 Feb 20;581(4):673-680.

9 Cines DB, Pollak ES, Buck CA, Loscalzo J, Zimmerman GA, McEver RP et al. Endothelial cells in physiology and in the pathophysiology of vascular disorders. Blood. 1998 May 15;91(10):3527-3561.

10 Dai G, Kaazempur-Mofrad MR, Natarajan S, Zhang Y, Vaughn S, Blackman BR et al. Distinct endothelial phenotypes evoked by arterial waveforms derived from atherosclerosis-susceptible and -resistant regions of human vasculature. Proc Natl Acad Sci U S A. 2004 Oct 12;101(41):14871-14876.

11 Davies PF, Tripathi SC. Mechanical stress mechanisms and the cell. An endothelial paradigm. Circ Res. 1993 Feb;72(2):239-245.

12 Dimmeler S, Assmus B, Hermann C, Haendeler J, Zeiher AM. Fluid shear stress stimulates phosphorylation of Akt in human endothelial cells: involvement in suppression of apoptosis. Circ Res. 1998 Aug 10;83(3):334-341.

13 Dimmeler S, Fleming I, Fisslthaler B, Hermann C, Busse R, Zeiher AM. Activation of nitric oxide synthase in endothelial cells by Akt-dependent phosphorylation. Nature. 1999 Jun 10;399(6736):601-605.

14 Drab M, Verkade P, Elger M, Kasper M, Lohn M, Lauterbach B et al. Loss of caveolae, vascular dysfunction, and pulmonary defects in caveolin-1 gene-disrupted mice. Science. 2001 Sep 28;293(5539):2449-2452.

15 Gouverneur M, Spaan JA, Pannekoek H, Fontijn RD, Vink H. Fluid shear stress stimulates incorporation of hyaluronan into endothelial cell glycocalyx. Am J Physiol Heart Circ Physiol. 2006 Jan;290(1):H458-462.

16 Gouverneur M, Van den Berg B, Nieuwdorp M, Stroes E, Vink H. Vasculoprotective properties of the endothelial glycocalyx: effects of fluid shear stress. Journal of Internal Medicine 2006; 259; 393-400

17 Habazettl H, Kukucka M, Weng YG, Kuebler WM, Hetzer R, Kuppe H et al. Arteriolar blood flow pulsatility in a patient before and after implantation of an axial flow pump. Ann Thorac Surg 2006 March; 81(3):1109-1111.

18 Hohberg M, Knöchel J, Hoffmann CJ, Chlench S, Wunderlich W, Alter A, et al. Expression of ADAMTS1 in endothelial cells is induced by shear stress and suppressed in sprouting capillaries. J Cell Physiol. 2011 Feb; 226(2):350-61.

19 Hsieh HJ, Li NQ, Frangos JA. Shear stress increases endothelial platelet-derived growth factor mRNA levels. Am J Physiol.1991 Feb;260(2Pt2):H642-646.

20 Itano N, Sawai T, Yoshida M, Lenas P, Yamada Y, Imagawa M et al. Three isoforms of mammalian hyaluronan synthases have distinct enzymatic properties. J Biol Chem. 1999 Aug 27;274(35):25085-25092.

21 Jaffe EA, Nachman RL, Becker CG, Minick CR. Culture of human endothelial cells derived from umbilical veins. Identification by morphologic and immunologic criteria. J Clin Invest. 1973 Nov;52(11):2745-56.

22 Kelly RF, Snow HM. Characteristics of the response of the iliac artery to wall shear stress in the anaesthetized pig. J Physiol. 2007 Jul 15;582(Pt 2):731-743.

23 Laemmli. Cleavage of structural proteins during the assembly of the head of bacteriophage T4. UK et al. Nature. (1970).

24 Lakota K, Mrak-Poljsak K, Rozman B, Sodin-Semrl S. Increased responsiveness of human coronary artery endothelial cells in inflammation and coagulation. Mediators Inflamm. 2009;2009:146872.

25 Laurent T.C., Fraser J.R. Hyaluronan. Faseb J. 1992 Apr;6(7):2397-2404.

26 Lehoux S, Castier Y, Tedgui A. Molecular mechanisms of the vascular responses to haemodynamic forces. J Intern Med. 2006 Apr;259(4):381-392.

27 Li YS, Haga JH, Chien S. Molecular basis of the effects of shear stress on vascular endothelial cells. J Biomech. 2005 Oct;38(10):1949-1971.

28 Lin MC, Almus-Jacobs F, Chen HH, Parry GC, Mackman N, Shyy JY et al. Shear stress induction of the tissue factor gene. J Clin Invest. 1997 Feb 15;99(4):737-744.

29 Lindert J, Werner J, Redlin M, Kuppe H, Habazettl H, Pries AR. OPS imaging of human microcirculation: a short technical report. J Vasc Res.2002 July;39(4):368-372.

30 Loufrani L, Retailleau K, Bocquet A, Dumont O, Danker K, Louis H et al. Key role of alpha(1)beta(1)-integrin in the activation of PI3-kinase-Akt by flow (shear stress) in resistance arteries. Am J Physiol Heart Circ Physiol. 2008 Apr;294(4):H1906-1913.

31 Mochizuki S, Vink H, Hiramatsu O, Kajita T, Shigeto F, Spaan JA, Kajiya F. Role of hyaluronic acid glycosaminoglycans in shear-induced endothelium-derived nitric oxide release. Am J Physiol Heart Circ Physiol. 2003 Aug;285(2):H722-726.

32 Nagy N, Freudenberger T, Melchior-Becker A, Röck K, Braak M, Jastrow H et al.. Inhibition of Hyaluronan Synthesis Accelerates Murine Atherosclerosis. Novel Insights Into the Role of Hyaluronan Synthesis. Circulation. 2010;122:2313-2322.

33 Nieuwdorp M, Holleman F, de Groot E, Vink H, Gort J, Kontush A et al. Perturbation of hyaluronan metabolism predisposes patients with type 1 diabetes mellitus to atherosclerosis. Diabetologia. 2007 Jun;50(6):1288-1293.

34 Noble MI, Drake-Holland AJ, Vink H. Hypothesis: arterial glycocalyx dysfunction is the first step in the atherothrombotic process. QJM. 2008 Jul;101(7):513-518.

35 Pahakis MY, Kosky JR, Dull RO, Tarbell JM. The role of endothelial glycocalyx components in mechanotransduction of fluid shear stress. Biochem Biophys Res Commun. 2007 Mar 30;355(1):228-233.

36 Papadaki M, Eskin SG. Effects of fluid shear stress on gene regulation of vascular cells. Biotechnol Prog. 1997 May-Jun;13(3):209-221.

37 Potter D.R. and Damiano E.R. The Hydrodynamically Relevant Endothelial Cell Glycocalyx Observed In Vivo Is Absent In Vitro. Circulation Research. 2008;102:770

38 Pries AR, Secomb TW, Gaehtgens P. The endothelial surface layer. Pflugers Arch. 2000 Sep;440(5):653-66. Review.

39 Reitsma S., Slaaf D.W., Vink H. The endothelial glycocalyx: composition, functions and visualization. Pflugers Arch. Eur J Physiol (2007) 454:345-359.

40 Secomb T.W., Hsu R., Pries A.R. Effect of the endothelial surface layer on transmission of fluid shear stress on endothelial cells. Biorheology. 2001;38(2-3):143-150.

41 Seog J, Dean D, Rolauffs B, Wu T, Genzer J, Plaas AH et al. Nanomechanics of opposing glycosaminoglycan macromolecules. J Biomech. 2005 Sep;38(9):1789-1797.

42 Shyy JY, Chien S. Role of integrins in endothelial mechanosensing of shear stress. Circ Res. 2002 Nov 1;91(9):769-775.

43 Shyy YJ, Hsieh HJ, Usami S, Chien S. Fluid shear stress induces a biphasic response of human monocyte chemotactic protein 1 gene expression in vascular endothelium. Proc Natl Acad Sci U S A. 1994 May 24;91(11):4678-4682.

44 Suzuki K, Yamamoto T, Usui T, Suzuki K, Heldin P, Yamashita H. Expression of Hyaluronan Synthase in Intraocular Proliferative Diseases: Regulation of Expression in Human Vascular Endothelial Cells by Transforming Growth Factor-β. Jpn J. Ophthalmol. 2003 Nov-Dec; 47(6) : 557-564

45 Tarbell J.M. & Pahakis M.Y. Mechanotransduction and the glycocalyx. J Intern Med 2006; 259; 339-350

46 Topper JN, Cai J, Falb D, Gimbrone MA Jr. Identification of vascular endothelial genes differentially responsive to fluid mechanical stimuli: cyclooxygenase-2, manganese superoxide dismutase, and endothelial cell nitric oxide synthase are selectively up-regulated by steady laminar shear stress. Proc Natl Acad Sci U S A. 1996 Sep 17;93(19):10417-10422.

47 Traub O, Berk BC. Laminar shear stress: mechanisms by which endothelial cells transduce an atheroprotective force. Arterioscler Thromb Vasc Biol. 1998 May;18(5):677-85.

48 van den Berg BM, Spaan JA, Rolf TM, Vink H. Atherogenic region and diet diminish glycocalyx dimension and increase intima-to-media ratios at murine carotid artery bifurcation. Am J Physiol Heart Circ Physiol. 2006 Feb;290(2):H915-920.

49 van den Berg BM, Spaan JA, Vink H. Impaired glycocalyx barrier properties contribute to enhanced intimal low-density lipoprotein accumulation at the carotid artery bifurcation in mice. Pflugers Arch. 2009 Apr;457(6):1199-1206.

50 van der Berg BM, Vink H, Spaan JA. The endothelial glycocalyx protects against myocardial edema. Circ Res. 2003 Apr 4; 92(6): 592-594

51 Weigel P. Bacterial Hyaluronan Synthases. 1998 Sep.

52 Weinbaum S, Tarbell JM, Damiano ER. The structure and function of the endothelial glycocalyx layer. Annu Rev Biomed Eng. 2007;9:121-167.

53 Wissler RW, Strong JP. Risk factors and progression of atherosclerosis in youth. PDAY Research Group. Pathological Determinants of Atherosclerosis in Youth. Am J Pathol. 1998 Oct;153(4):1023-1033.

54 Woolf N., The arterial endothelium. Pathology of atherosclerosis. London: Butterworths, 1982, p. 25-45

55 Yoshizumi M, Abe J, Tsuchiya K, Berk BC, Tamaki T. Stress and vascular responses: atheroprotective effect of laminar fluid shear stress in endothelial cells: possible role of mitogen-activated protein kinases. J Pharmacol Sci. 2003 Mar;91(3):172-176.

List of publications

1. Hohberg M, Knöchel J, Hoffmann CJ, Chlench S, Wunderlich W, Alter A, Maroski J, Vorderwülbecke BJ, Da Silva-Azevedo L, Knudsen R, Lehmann R, Fiedorowicz K, Bongrazio M, Nitsche B, Hoepfner M, Styp-Rekowska B, Pries AR, Zakrzewicz A. Expression of ADAMTS1 in endothelial cells is induced by shear stress and suppressed in sprouting capillaries. J Cell Physiol. 2011 Feb; 226(2):350-61.
2. Hoffmann CJ, Hohberg M, Chlench S, Maroski J, Drab M, Siegel G, Pries AR, Zakrzewicz A. Suppression of zinc finger protein 580 by high oxLDL/LDL-ratios is followed by enhanced expression of endothelial IL-8. Atherosclerosis. 2011 May;216(1):103-8.
3. Maroski J, Vorderwülbecke BJ, Fiedorowicz K, Da Silva-Azevedo L, Siegel G, Marki A, Pries AR, Zakrzewicz A. Shear stress increases endothelial hyaluronan synthase 2 and hyaluronan synthesis especially in regard to an atheroprotective flow profile. Exp Physiol. 2011 Sep;96(9):977-86.
4. Vorderwülbecke BJ, Maroski J, Fiedorowicz K, Da Silva-Azevedo L, Marki A, Pries AR, Zakrzewicz A. Regulation of endothelial connexin40 expression by shear stress. Am J Physiol Heart Circ Physiol. 2012 Jan;302(1):H143-52.
5. Zakrzewicz A, Maroski J, Vorderwülbecke BJ, Silva-Azevedo LD, Fiedorowicz K, Pries AR. Endothelial hyaluronan synthase 2 and hyaluronan are increased by an atheroprotective flow profile. Cardiovascular Research. Frontiers in Cardiovascular Biology. Berlin 2010 Jul. Poster presentation.
6. Zakrzewicz A, Hoffmann CJ, Hohberg M, Chlench S, Maroski J, Siegel G, Drab M, Pries AR. Zinc finger protein S80: A novel factor in endothelial pathway distinct for lipoprotein-induced response of IL 8. Cardiovascular Research. Frontiers in Cardiovascular Biology. Berlin 2010 Jul. Poster presentation.
7. Maroski J, Vorderwülbecke BJ, Silva-Azevedo LD, Pries AR, Zakrzewicz A. Shear stress-dependent effects on endothelial hyaluronan synthase 2. Acta Physiologica. 87th annual meeting. Deutsche Physiologische Gesellschaft. 2010 March. Poster presentation.
8. Vorderwülbecke BJ, Maroski J, Silva-Azevedo LD, Pries AR, Zakrzewicz A. Shear stress regulates endothelial connexin 40 by a PI3-kinase dependent pathway. Acta Physiologica. 87th annual meeting. Deutsche Physiologische Gesellschaft. 2010 March. Poster presentation.

Erklärung

„Ich, Julian Maroski, erkläre, dass ich die vorgelegte Dissertation mit dem Thema: *Hyaluronan synthase 2 and hyaluronan in endothelial cells are increased by shear stress via the PI3-kinase-Akt-pathway with the most pronounced effect by an atheroprotective flow profile.* selbst verfasst und keine anderen als die angegebenen Quellen und Hilfsmittel benutzt, ohne die (unzulässige) Hilfe Dritter verfasst und auch in Teilen keine Kopien anderer Arbeiten dargestellt habe.“

Berlin, 22.01.2013

Lebenslauf

(Mein Lebenslauf wird aus datenschutzrechtlichen Gründen in der elektronischen Version meiner Arbeit nicht veröffentlicht.)